

Numerical analysis of vertical drains accelerated consolidation considering combined soil disturbance and visco-plastic behaviour

Babak Azari^a, Behzad Fatahi^{*} and Hadi Khabbaz^b

Faculty of Engineering and IT, University of Technology Sydney, Australia

(Received August 14, 2014, Revised November 13, 2014, Accepted November 15, 2014)

Abstract. Soil disturbance induced by installation of mandrel driven vertical drains decreases the in situ horizontal hydraulic conductivity of the soil in the vicinity of the drains, decelerating the consolidation rate. According to available literature, several different profiles for the hydraulic conductivity variation with the radial distance from the vertical drain, influencing the excess pore water pressure dissipation rate, have been identified. In addition, it is well known that the visco-plastic properties of the soil also influence the excess pore water pressure dissipation rate and consequently the settlement rate. In this study, a numerical solution adopting an elastic visco-plastic model with nonlinear creep function incorporated in the consolidation equations has been developed to investigate the effects of disturbed zone properties on the time dependent behaviour of soft soil deposits improved with vertical drains and preloading. The employed elastic visco-plastic model is based on the framework of the modified Cam-Clay model capturing soil creep during excess pore water pressure dissipation. Besides, nonlinear variations of creep coefficient with stress and time and permeability variations during the consolidation process are considered. The predicted results have been compared with Väsby test fill measurements. According to the results, different variations of the hydraulic conductivity profile in the disturbed zone result in varying excess pore water pressure dissipation rate and consequently varying the effective vertical stresses in the soil profile. Thus, the creep coefficient and the creep strain limit are notably influenced resulting in significant changes in the predicted settlement rate.

Keywords: numerical analysis; consolidation; visco-plastic behaviour; creep; vertical drains; soil disturbance; preloading; post-construction settlement

1. Introduction

The population growth, the urbanisation development and as a result the infrastructure progression such as highways, railways and ports have increased the need of appropriate ground for living and development more than ever. Consequently, many other land sources even with poor bearing capacity such as the waterside areas alongside lakes, rivers, and marine shores are being contemplated by developers. The prevalent soils in these areas, considered as soft soils, are

*Corresponding author, Senior Lecturer of Geotechnical Engineering, E-mail: Behzad.Fatahi@uts.edu.au

^a Ph.D. Candidate, E-mail: Babak.Azari@student.uts.edu.au

^b Associate Professor of Geotechnical Engineering, E-mail: Hadi.Khabbaz@uts.edu.au

characterised by the low shear strength, the high compressibility, and the low hydraulic conductivity. One of the main challenges of clients and designers is minimising the future maintenance costs associated with the long-term performance of structures constructed on soft soils. For example, investigating the long-term behaviour (e.g., settlement and lateral deformation) of soft soils under highway or railway embankments is a challenging task for geotechnical engineers. In addition, soft soils may significantly change performance of superstructures while subjected to earthquakes due to large foundation deformations (e.g., Fatahi and Tabatabaiefar 2014, Hokmabadi *et al.* 2014a, b, Tabatabaiefar *et al.* 2013a, b, Tabatabaiefar and Fatahi 2014).

Post-construction deformation of soft soils including clays, silts and peats, may be extreme during the life time of the structure. Therefore, in order to minimise the post-construction settlement and improve the bearing capacity and the shear strength of the soft soil deposits, various methods such as soil cementation, addition of fibre (Fatahi *et al.* 2013) or preloading combined with vertical drains may be used. Preloading comprises of applying a load, equal to or greater than the entire load of a planned structure, over the site earlier than constructing the structure. Preloading, which is commonly an earth fill, applies compression to the underlying soil, which is being partially or fully removed while the required settlement has taken place.

Prefabricated vertical drains (PVDs) are installed using closed end mandrels. Mandrel insertion causes soil disturbance in the vicinity of the drain. The disturbed zone around the vertical drain possessing reduced hydraulic conductivity in the horizontal direction, can remarkably affect the excess pore water pressure dissipation rate and the creep coefficient (Holtz and Holm 1973, Lo and Mesri 1994, Bergado *et al.* 1991, Sharma and Xiao 2000, Basu and Prezzi 2007, Walker and Indraratna 2006, Parsa-Pajouh *et al.* 2014).

Numerous studies have been carried out to investigate the consolidation of saturated and unsaturated soils (Ho *et al.* 2014, Qin *et al.* 2014). The mechanical response of soft soils such as inelastic behaviour under loading is significantly influenced by clay, the major composition of soft soils, which has sophisticated mineralogical composition and structure (Shen *et al.* 2012, Nguyen *et al.* 2014). Creep (time dependant viscous behaviour of soil) is a significant part of the soft soil settlement which may cause substantial deformation in the long-term. Creep deformation may be considered as destruction or adjustment of the soil structure under a constant effective stress. The explanation of the mechanism of creep settlement based on the clay mineralogy as well as the deformation of both macro and microstructures of soils can be relevant to employ for settlement prediction. In the macroscopic view, creep deformation is the result of the rearrangement or adjustment of soil structural to reach a new equilibrium under an applied stress. In the microscopic level, creep deformation is described as the deformation of microstructure (clay minerals and absorbed water layer) due to the drainage pore fluid in micropores, or due to the structural viscosity of pore fluids (Mitchell 1956, Bjerrum 1967, Le *et al.* 2012, Azari *et al.* 2014, Le *et al.* 2015). By and large, viscous creep is an area that has been ignored even in the most recent constitutive and numerical models used to simulate consolidation of soft soils with both vertical and radial drainage (e.g., Bergado *et al.* 1992, Hird *et al.* 1992, Hong and Shang 1998, Indraratna *et al.* 2005, Xie *et al.* 2012).

Mesri and Feng (1991) proposed a creep ratio concept to simulate the behaviour of preloaded soft soils. Furthermore, Mesri (1986) interpreted post-surcharge compression behaviour of soft soils in relationship with the compression index. Although the creep ratio concept is practical, it has some limitations including lack of excess pore water pressure simulation, difficulties with numerical calculations, while considering the nonlinear variation of permeability with void ratio influencing the excess pore water pressure dissipation rate. Furthermore, Mesri *et al.* (1975)

reported the compression index, used in the creep ratio concept, as a function of the vertical effective stress during consolidation process which results in difficulties in determining the compression index.

Barron (1948) and Hansbo (1981) developed theoretical studies on soil disturbance with the assumption of a radial flow of water into the drain. Their solutions can be applied to estimate the degree of consolidation as a function of time. A vertical drain with a circular cross-section is considered in those formulations. Barron (1948) obtained the solution based on the Terzaghi-Rendulic theory of radial consolidation (Terzaghi 1925, Rendulic 1935, 1936), whereas Hansbo (1981) obtained the solution based on the continuity of flow and Darcy's law. The solution obtained by Hansbo (1981) matches closely the Barron (1948) solution and is broadly used in practice. Walker and Indraratna (2006) presented an axisymmetric drain radial consolidation equation based on parabolic reduction pattern in the permeability toward the drain. The calculation procedure similar to Hansbo (1981) axisymmetric solution was adopted with modification, in order to incorporate the decay of permeability in the disturbed zone. Hansbo's (1981) equations calculate the settlement based on the vertical effective stress values at a given time, and as a result, it cannot capture the effects of time dependant viscous behaviour of the soil. Moreover, although the real soft soil properties keep changing during the consolidation process, Walker and Indraratna (2006) assumed that soil parameters (e.g., soil permeability, vertical coefficient of consolidation in intact and disturbed zones, and coefficient of volume compressibility in intact and disturbed zones) stay constant during the consolidation process. Basu *et al.* (2006, 2010) developed analytical solutions for consolidation of soft soils improved by vertical drains, considering both disturbed and transition zones using a methodology similar to that of Hansbo (1981). Although they considered five different patterns for hydraulic conductivity variations in disturbed zone to obtain the analytical solutions, the time dependant viscous behaviour of soft soils was not considered. Furthermore, results were normalized by the final settlement when the excess pore water pressure is equal to zero. It should be mentioned that since creep occurs concurrently with the excess pore water pressure dissipation process, considering identical final settlements for all five different situations may not be accurate. Zhu and Yin (2000) combined the continuity and the constitutive effective stress-strain equations to simulate the deformation of soft soils improved with vertical drains. Their proposed simplified finite element method has been efficient for the consolidation analysis of soils with vertical drain and preloading. That simplified method formulation can be applied to layered soil, time-dependent loading, capturing the disturbance effect and inelastic stress-strain behaviour. They employed the conventional consolidation theory developed by Terzaghi (1941) and Barron (1948) and therefore neglected viscous/creep behaviour of the soil during the consolidation process (Zhu and Yin 2000). Nash and Ryde (2001) developed a one dimensional finite difference consolidation analysis which is capable of considering multi-layer soil profile, disturbed zone, and permeability variation based on void ratio. They applied the original elastic visco-plastic proposed by Yin (1990) for the finite different solution and consequently ignored the creep strain limit and nonlinearity of creep coefficient.

Based on the available literature, there is a lack of consideration with respect to the combined effects of the hydraulic conductivity profile in disturbed zone and the nonlinear visco-plastic behaviour of soil influencing the creep parameters and settlement rate and consequently deformation of soft soils improved using vertical drains (Zhu and Yin 2000, Walker and Indraratna 2006, Basu *et al.* 2006, 2010). According to the fact that different hydraulic conductivities in the disturbed zone may result in different settlement, consolidation and creep coefficients at any given time in the soil profile, effects of the hydraulic conductivity variations in the disturbed zone on the

settlement prediction should be evaluated more carefully.

In this paper, the elastic visco-plastic model, considering a nonlinear creep function and creep strain limit, developed by Yin and Graham (1989), is incorporated in the consolidation equation to investigate the effects of soil disturbance induced by the installation of prefabricated vertical drains (PVDs) on time dependant performance of soft soil deposits. Finite difference formulations for fully coupled one dimensional axisymmetric consolidation are adopted to model the time dependent behaviour of the soft soil combining both vertical and radial drainage, and variations of the settlement and the excess pore water pressures of the ground with time are reported. Different possible variations of the horizontal permeability in the disturbed zone and nonlinear variations of the permeability with void ratio changes in combination with the soil creep are considered. The effects of different hydraulic conductivity profiles on settlement, the excess pore water pressure dissipation rate, the creep coefficient, and the creep strain limit are investigated and discussed for Väsby test fill, built in Sweden, with settlement data available for 20 years, as a case study.

2. Elastic visco-plastic behaviour of soils

Different approaches have been proposed to estimate the time dependant deformation of soft soils. In general, researchers suggest two broad concepts: (i) although creep occurs during the excess pore water pressure dissipation (known as primary consolidation process), the void ratio when the excess pore water pressure has fully dissipated at the end of primary consolidation (e_{EOP}) is unique for thin and thick samples and all the subsequent calculations are based on this assumption (Hypothesis A) (e.g., Ladd 1973, Ladd *et al.* 1977, Mesri 2001, Mesri and Feng 1991, Mesri *et al.* 1994); and (ii) considering the fact that primary consolidation consists of creep deformation, which is increasing with time, the value of e_{EOP} for thin and thick soil samples cannot be unique and the equations should embrace the results of this assumption (Hypothesis B) (e.g., Suklje 1957, Barden 1965, 1969, Bjerrum 1967, Yin and Graham 1989, 1994). In Hypothesis A, soil settlement is divided into two parts, primary consolidation (during dissipation of excess pore water pressure) followed by the secondary compression (while the remaining excess pore water pressure left is insignificant). However, in Hypothesis B, soil settlement is estimated using an elastic visco-plastic constitutive model simulating creep deformation and excess pore water pressure dissipation simultaneously and continuously.

Bjerrum (1967) represented a relationship between the applied stresses, compression and time, by a system of lines, while each line being a representative of a unique relationship between stress, strain and time. Time line system concept of Bjerrum (1967) was adopted by Yin (1990) assuming that time lines are lines with the same values of "equivalent times" (t_e). However, as explained by Yin (1999), unlike Bjerrum's (1967) concept, each time line can be correlated to a unique creep coefficient and it is not necessarily equal to the loading duration. The time line concept comprises an instant time line, a reference time line, a limit time line, and a set of equivalent time lines. Fig. 1 depicts schematic fitting curves for instant, reference, equivalent, and limit time lines.

As described by Yin and Graham (1989), the instant time line defines the elastic-plastic settlement and is correlated to the normal consolidation line. Nevertheless, instant compression is expressed by Yin (1990) as time independent elastic compression. As explained by Yin *et al.* (2002), the normal consolidation or overconsolidation lines are often generated by the standard oedometer tests which may include creep deformation (while excess pore water pressure is being dissipated) since the consecutive loadings in the tests are generally kept constant for 24 hours. As

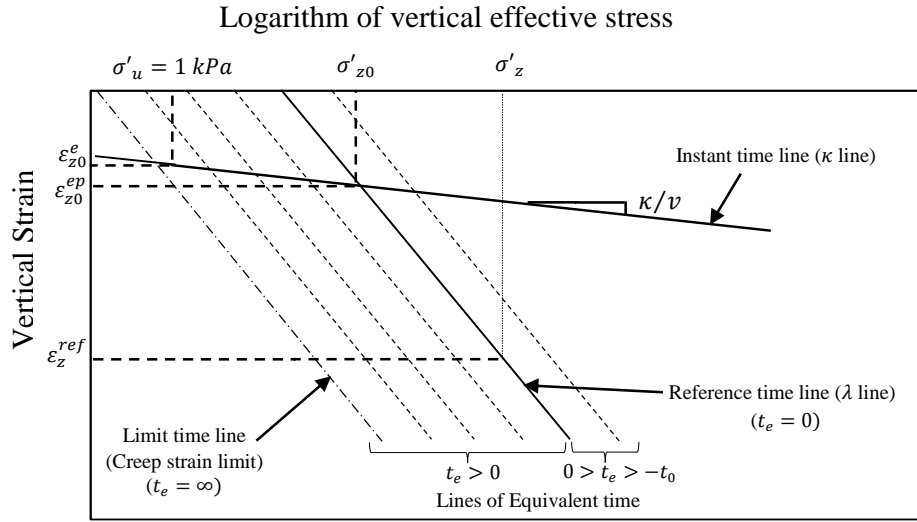


Fig. 1 Schematic fitting curves for instant, reference, equivalent and limit time lines

a result, the true instant line should be obtained by reloading/unloading tests. The instant time line fitting equation can be defined as follows

$$\varepsilon_z^e = \varepsilon_{z0}^e + \frac{k}{v} \ln \left(\frac{\sigma'_z}{\sigma'_u} \right) \quad (1)$$

where, σ'_u is a unit stress, ε_z^e is the vertical strain at stress level σ'_z , ε_{z0}^e is the vertical strain at $\sigma'_z = \sigma'_u$, and k/v is a material parameter describing the elastic stiffness of the soil, in which v is the specific volume ($v = 1 + e_0$), and e_0 is the initial void ratio.

Yin and Graham (1989) proposed their original elastic visco-plastic model assuming the creep coefficient is constant. However, according to the field measurements and laboratory test results (e.g., Yin 1999, Mesri 2001, Yin *et al.* 2002) the relationship between the strain (or void ratio) and logarithm of time is not linear. Consequently, in order to simulate the behaviour of soft soils more accurately, Yin (1999) proposed a modified creep function incorporating a nonlinear creep coefficient and the creep strain limit.

The authors believe that there is an absolute minimum value for the volume of solid in a soil element while no void exists within that soil element. As expressed by Mitchell (1956), regardless of the pressure or initial orientation, void ratio for a particular soil can reach to a minimum value. It means that the soil structure cannot deform forever. Thus, the deformation of soils under a particular applied pressure must cease after a finite period that can be counted in years or decades, meaning that there is a finite strain. The compression may end under the final effective stress that the ultimate equilibrium inside the soil structure is reached or when no void and fluid exist inside the clay particles. Obviously, creep strain limit measurement is not an easy task since it is not feasible to carry out the tests for infinity duration. Hence, it can be assumed that the limit strain can be reached when the volume of voids within the soil approaches zero under the applied stress at the infinity time. Yin *et al.* (2002) proposed that the creep strain limit may be estimated based on the initial void ratio as follows

$$\varepsilon_{cr}^{limit} = \frac{e_0}{1 + e_0} \quad (2)$$

where, ε_{cr}^{limit} is the creep strain limit and e_0 is the initial soil void ratio.

However, the authors believe that Eq. (2) is an overestimation of the creep strain limit since the term $e_0 / 1 + e_0$ consists of the conventional consolidation volume change due to hydrodynamic excess pore water pressure dissipation as well as the creep. As a result, the soil void ratio at a certain effective stress on the reference time line should be used to define the creep strain limit for a particular applied effective stress as follows

$$\varepsilon_{cr}^{limit} = \frac{e_{ref}}{1 + e_0} \quad (3)$$

where

$$e_{ref} = \left(\varepsilon_z - \frac{\lambda}{v} \ln \left(\frac{\sigma'_z}{\sigma'_{z0}} \right) \right) (1 + e_0) + e_z \quad (4)$$

where, e_{ref} is the void ratio at effective stress equal to σ'_z on the reference time line, ε_z is the soil vertical strain, σ'_{z0} is a material property, and e_z is the void ratio at a particular applied effective stress.

As stated by Yin and Graham (1989), the equivalent time line by some means is comparable to the equivalent pressure defined in the critical state soil mechanics. The equivalent time (t_e) is referred to the time that young clay needs to wait after instantaneous loading along the reference line (λ line) to get to the required future state point condition. The time needed for soil to creep from the reference time line to a state point under the same effective stress is defined by Yin (1999) as the equivalent time (t_e). As explained by Yin *et al.* (2002), an equivalent time (t_e) can be defined as a function of the state point (σ'_z, ε_z), as follows

$$t_e = -t_0 + t_0 \exp \left[\frac{\varepsilon_z - \varepsilon_{z0}^{ep} - \frac{\lambda}{v} \ln \left(\frac{\sigma'_z}{\sigma'_{z0}} \right)}{\frac{\psi_0}{v} \left(1 - \frac{\varepsilon_z - \varepsilon_{z0}^{ep} - \frac{\lambda}{v} \ln \left(\frac{\sigma'_z}{\sigma'_{z0}} \right)}{\varepsilon_{cr}^{limit}} \right)} \right] \quad (5)$$

where, t_0 , $\frac{\psi_0}{v}$, $\frac{\lambda}{v}$, and ε_{z0}^{ep} are curve-fitting parameter related to the choice of the reference time line, the initial creep coefficient, the elastic-plastic stiffness of the soil, and the vertical strain at $\sigma'_z = \sigma'_{z0}$, respectively.

Equivalent times above and below the reference time line are negative and positive,

respectively, as shown in Fig. 1. In overconsolidated range, equivalent time is a function of the consolidation ratio, however, in normally consolidation range and multistage loading tests (i.e., constant load increment), the equivalent time is usually equal to the duration of the load increment (Yin and Graham 1994). According to Yin *et al.* (2002), the vertical creep compression strain (ε_z^{vp}) can be calculated by the following equation

$$\varepsilon_z^{vp} = \frac{\psi}{v} \ln \left(\frac{t_0 + t_e}{t_0} \right) \quad \text{for } t_0 < t_e < \infty \quad (6)$$

where

$$\frac{\psi}{v} = \frac{\psi_0}{v} \ln \left(\frac{t_0 + t_e}{t_0} \right) \quad (7)$$

$$1 + \frac{\psi_0}{v \varepsilon_{cr}^{\text{limit}}}$$

where, $\frac{\psi}{v}$ is the creep coefficient, and $\frac{\psi_0}{v}$ is the initial value of $\frac{\psi}{v}$ at $t_e = 0$.

Yin (1990) defined the reference time line as the line with the equivalent time equal to zero ($t_e = 0$). The reference line can be used to calculate the equivalent time, and reasonably can be taken as the line with no excess pore water pressure or at “some other time” to calculate the creep strains (Yin 1990). As explained by Yin and Graham (1994), in time independent soils, while viscosity of the soil is equal to zero, the reference time line is the elastic-plastic line. The fitting function for the reference time line can be presented as

$$\varepsilon_z^{ep} = \varepsilon_{z0}^{ep} + \frac{\lambda}{v} \ln \left(\frac{\sigma'_z}{\sigma'_{z0}} \right) \quad (8)$$

As suggested by Yin and Graham (1994), a unique limit time line in the space of $(\sigma'_z, \varepsilon_z)$ exists for both viscous and non-viscous soils. They expressed the limit time line as the line which has $t_e = \infty$ and the creep coefficient of zero. Behaviour of the soil beyond the limit time line is time independent. It is believed that the creep straining will finally terminate after very long time (infinity) when the soil particles occupy a fixed volume. The fitting function for the limit time line is as follows

$$\varepsilon_z^{\text{limit}} = \varepsilon_{z0}^{ep} + \frac{\lambda}{v} \ln \left(\frac{\sigma'_z}{\sigma'_{z0}} \right) + \varepsilon_{cr}^{\text{limit}} \quad (9)$$

where, $\varepsilon_z^{\text{limit}}$ is the strain limit, and ε_{z0}^{ep} is the initial strain on the reference time line.

According to Yin *et al.* (2002), considering and combining Eqs. (1) to (9), the elastic viscoplastic model to predict the time dependant behaviour of soft soils can be obtained using Eqs. (10) and (11)

$$\left\{ \begin{array}{l} \frac{\partial \varepsilon_z}{\partial t} = \frac{\kappa}{v \sigma'_z} \frac{\partial \sigma'_z}{\partial t} \quad \text{for } (\sigma'_z, \varepsilon_z) \text{ below the limit timeline} \end{array} \right. \quad (10a)$$

$$\left\{ \begin{array}{l} \frac{\partial \varepsilon_z}{\partial t} = \frac{\kappa}{v \sigma'_z} \frac{\partial \sigma'_z}{\partial t} + g(\sigma'_z, \varepsilon_z) \quad \text{for } (\sigma'_z, \varepsilon_z) \text{ above the limit timeline} \end{array} \right. \quad (10b)$$

where

$$g(\sigma'_z, \varepsilon_z) = \frac{\psi_0}{vt_0} \left(\frac{\varepsilon_{z0}^{ep} + \frac{\lambda}{v} \ln\left(\frac{\sigma'_z}{\sigma'_{z0}}\right) - \varepsilon_z}{\varepsilon_{cr}^{limit}} \right)^2 \exp \left(\frac{v}{\psi_0} \frac{\varepsilon_{z0}^{ep} + \frac{\lambda}{v} \ln\left(\frac{\sigma'_z}{\sigma'_{z0}}\right) - \varepsilon_z}{1 + \frac{\varepsilon_{z0}^{ep} + \frac{\lambda}{v} \ln\left(\frac{\sigma'_z}{\sigma'_{z0}}\right) - \varepsilon_z}{\varepsilon_{cr}^{limit}}} \right) \quad (11)$$

Eqs. (10a) and (10b) represent the soil behaviour transition from heavily over-consolidated to lightly over-consolidated and finally normally consolidated situation. Eq. (10a) denotes the situation where the soil is heavily over-consolidated and as a result, the viscous creep component is insignificant, while Eq. (10b) denotes the situation where the soil is lightly over-consolidated or normally consolidated and consequently, the behaviour is a function of effective stress and time (Fig. 1). It should be noted that the above mentioned equations are in 1-D platform and can be used for one dimensional consolidation. Further explanation regarding equations in 3-D can be found in Yin *et al.* (2002).

3. Soil disturbance induced during vertical drains installation

As mentioned earlier, prefabricated vertical drains are installed using: mandrel, disturbing the soil around the drain to a certain extent, and resulting in the reduction of the horizontal soil permeability in this region (Fig. 2). The extent of the soil hydraulic conductivity changes in the disturbed zone versus the distance from the vertical drain has not been identified with certainty and so far there is no comprehensive or standard method for measuring these characteristics. According to field and laboratory observations (e.g., Bergado *et al.* 1991, Madhav *et al.* 1993,

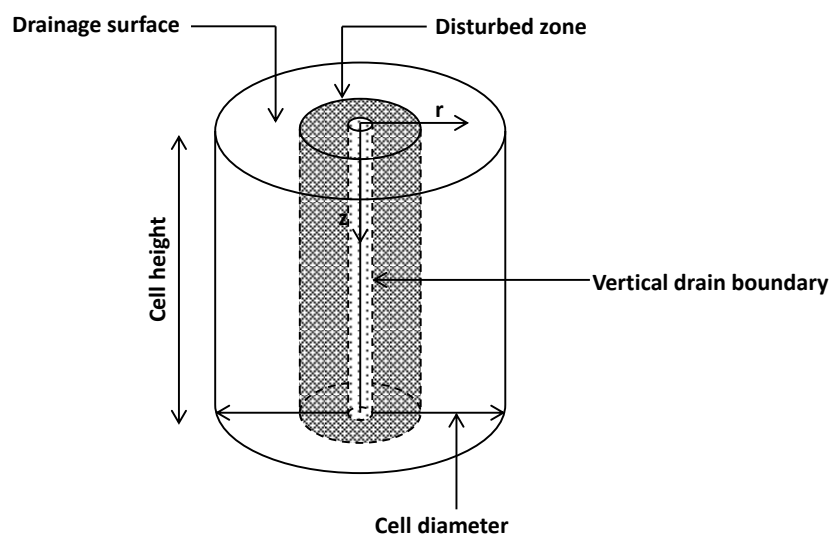


Fig. 2 Schematic 3D-axisymmetric consolidation

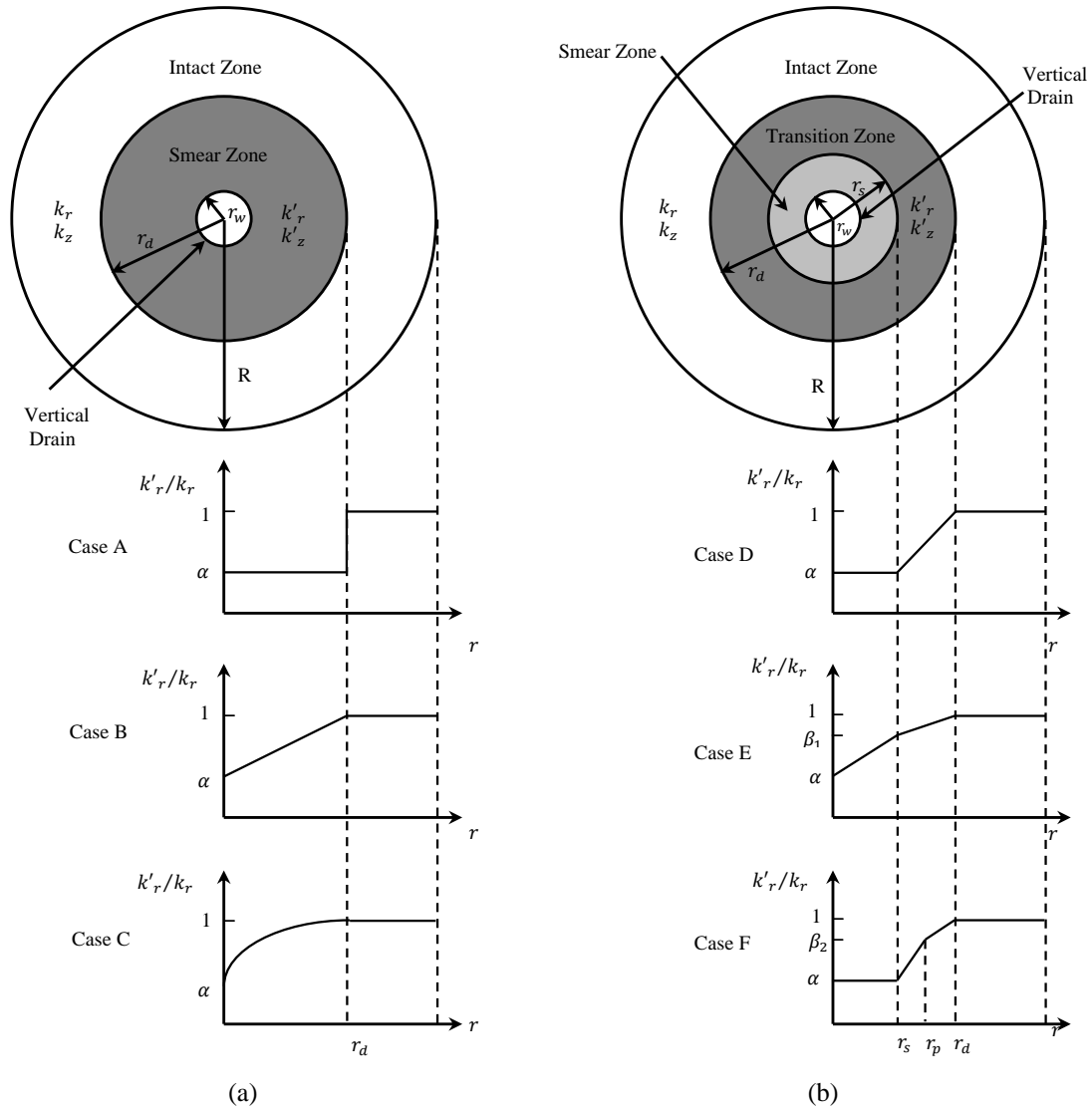


Fig. 3 Cross section of the disturbed zone surrounding a vertical drain: (a) two zones hypothesis; (b) three zones hypothesis

Indrarantna and Redana 1998b, Hird and Moseley 2000), the soil hydraulic conductivity varies with radial distance away from the vertical drain. Although some efforts have been made to simulate a gradual variation of the hydraulic conductivity with radius (Madlav *et al.* 1993, Chai *et al.* 1997, Hawlader *et al.* 2002), it has never been a straight forward task to quantify the disturbing effects (Hansbo 1997). In general, to characterise the disturbed zone, two major parameters including the permeability (k'_r), and the extent (r_d) of the disturbed zone are proposed. Bergado *et al.* (1991) stated that the vertical drains installation procedure, mandrel specifications and the type of soil are the key factors influencing the disturbed zone characteristics. According to Barron (1948), inserting and withdrawing cased holes, which are back filled, would distort and remould

Table 1 Various available permeability variation equations

Case	Suggested equations for permeability in disturbed zone	Reference
Case A	$k'_r(r) = k'_z(r) = \alpha k_h$	Barron (1948) Holtz and Holm (1973)
Case B	$k'_r(r) = k'_z(r) = k_r \left(\alpha + \left(\frac{1-\alpha}{r_d} \right) r \right)$	Rujikiatkamjorn and Indraratna (2009)
Case C	$k'_r(r) = k'_z(r) = k_r \left(\left(\frac{1-\alpha}{(r_d)^2} \right) r^2 + 2 \left(\frac{1-\alpha}{r_d} \right) r + \alpha \right)$	Walker and Indraratna (2006)
Case D	$k'_r(r) = k'_z(r) = \alpha k_r$	$0 < r < r_s$
	$k'_r(r) = k'_z(r) = k_r \left(\alpha + \frac{1-\alpha}{r_d} r \right)$	$r_s < r < r_d$
Case E	$k'_r(r) = k'_z(r) = k_r \left(\alpha + \left(\frac{\beta_1 - \alpha}{r_d} \right) r \right)$	$0 < r < r_s$
	$k'_r(r) = k'_z(r) = k_r \left(\beta_1 + \left(\frac{1-\beta_1}{r_d - r_s} \right) (r - r_s) \right)$	$r_s < r < r_d$
Case F	$k'_r(r) = k'_z(r) = \alpha k_r$	$0 < r < r_s$
	$k'_r(r) = k'_z(r) = k_r \left(\alpha + \left(\frac{\beta_2 - \alpha}{r_p - r_s} \right) (r - r_s) \right)$	$r_s < r < r_p$
	$k'_r(r) = k'_z(r) = k_r \left(\beta_2 + \left(\frac{1-\beta_2}{r_d - r_p} \right) (r - r_p) \right)$	$r_p < r < r_d$

the soil in the vicinity of the vertical drain. In general, researchers suggest two broad concepts to determine the characteristics of the soil surrounding the drain: (i) two zones hypothesis, consisting of the intact zone surrounding the disturbed zone adjacent to the vertical drain; and (ii) three zones hypothesis, comprised of the undisturbed zone surrounding the transition zone and the smear zone in the immediate vicinity of the vertical drain.

Based on the available literature (e.g., Barron 1948, Onoue *et al.* 1991, Madhav *et al.* 1993, Walker and Indraratna 2006, Basu *et al.* 2006, Rujikiatkamjorn and Indraratna 2009), various patterns have been proposed for the initial hydraulic conductivity of the soil in the disturbed region (Fig. 3).

According to most researchers (e.g., Barron 1948, Holtz and Holm 1973, Hansbo 1981, Jamiolkowski *et al.* 1983, Chai and Miura 1999), the soil inside the disturbed zone is entirely remoulded, causing an initial constant hydraulic conductivity which is smaller than the undisturbed horizontal hydraulic conductivity (Fig. 3(a), Case A). As stated by Rujikiatkamjorn

and Indraratna (2009), the initial hydraulic conductivity of the disturbed zone may have a linear variation with the radial distance (Fig. 3(a), Case B), while a parabolic distribution of the permeability in the disturbed region was proposed by Walker and Indraratna (2006) (Fig. 3(a), Case C). Madhav *et al.* (1993) proposed a constant hydraulic conductivity which is smaller than the undisturbed hydraulic conductivity in the smear zone and a linear hydraulic conductivity variation in the transition zone (Fig. 3(b), Case D). Onoue *et al.* (1991) proposed bilinear variation for the hydraulic conductivity, assuming permeability is changing linearly in the smear and the transition zones (Fig. 3(b), Case E). Furthermore, Basu *et al.* (2006) assumed that the horizontal hydraulic conductivity is constant in the smear zone and proposed bilinear variation of the permeability in the transition zone (Fig. 3(b), Case F). Table 1 summarises various available permeability variation equations for disturbed zone corresponding to different patterns presented in Fig. 3.

4. Finite difference solution of axisymmetric consolidation equation

Barron (1948) proposed the governing equation for estimation of one dimensional axisymmetric consolidation deformation of a saturated soil considering both vertical and horizontal drainage as shown in Eq. (12). The assumptions to obtain this equation are: (i) the soil is completely saturated; (ii) water and soil particles are incompressible; (iii) Darcy's law is valid; and (iv) strains are small. Obviously, when the soil consists of horizontal layers with thickness (or the length of vertical drains) of much lesser than the dimensions of the preloading area, or for the points located at the centre of the embankment, the average strain or deformation of the soil can be calculated using 1D (vertical) assumption reasonably accurate.

$$-\frac{\partial \varepsilon_z}{\partial t} = \frac{k_r}{\gamma_w} \left(\frac{\partial^2 u}{\partial r^2} + \frac{1}{r} \frac{\partial u}{\partial r} \right) + \frac{k_z}{\gamma_w} \left(\frac{\partial^2 u}{\partial z^2} \right) \quad (12)$$

where, ε_z and σ_z are the vertical strain and total stress, respectively, k_r and k_z are the coefficients of permeability in horizontal and vertical directions, respectively, γ_w is the unit weight of water, u is the excess pore water pressure at time t , and r and z are the radial and vertical coordinates, respectively.

As shown in Eq. (12), the hydraulic conductivity profile in the vicinity of the drain (k_r) is one of the key parameters influencing the consolidation rate and consequently the required preloading time which should be considered for ground improvement projects influencing the post-construction settlement of infrastructure.

Eqs. (10)-(12) and the effective stress concept of Terzaghi can be combined to predict the time dependent behaviour of the soil inside and outside of the disturbed zone (Eqs. (13) and (14)). Furthermore, defining equations based on the effective stresses in combination with the consolidation theory (Eq. (12)) facilitates to embrace the effects of excess pore water pressure on the settlement rate, while considering elastic visco-plastic behaviour of soils. It can be noted that the term $\frac{\partial \sigma_z}{\partial t}$ captures both time dependant loading and unloading processes (i.e., staged construction).

For the disturbed zone

(1) when $(\sigma'_z, \varepsilon_z)$ is below the limit time line

$$-\frac{\kappa}{v(\sigma'_z - u)} \left(\frac{\partial \sigma'_z}{\partial t} - \frac{\partial u}{\partial t} \right) = \frac{k'_r(r)}{\gamma_w} \left(\frac{\partial^2 u}{\partial r^2} + \frac{1}{r} \frac{\partial u}{\partial r} \right) + \frac{k'_z(r)}{\gamma_w} \left(\frac{\partial^2 u}{\partial z^2} \right) \quad (13a)$$

(2) when $(\sigma'_z, \varepsilon_z)$ is above the limit time line

$$-\frac{\kappa}{v(\sigma'_z - u)} \left(\frac{\partial \sigma'_z}{\partial t} - \frac{\partial u}{\partial t} \right) = \frac{k'_r(r)}{\gamma_w} \left(\frac{\partial^2 u}{\partial r^2} + \frac{1}{r} \frac{\partial u}{\partial r} \right) + \frac{k'_z(r)}{\gamma_w} \left(\frac{\partial^2 u}{\partial z^2} \right) + g(\sigma'_z, \varepsilon_z) \quad (13b)$$

For the intact zone

(1) when $(\sigma'_z, \varepsilon_z)$ is below the limit time lined

$$-\frac{\kappa}{v(\sigma'_z - u)} \left(\frac{\partial \sigma'_z}{\partial t} - \frac{\partial u}{\partial t} \right) = \frac{k_r}{\gamma_w} \left(\frac{\partial^2 u}{\partial r^2} + \frac{1}{r} \frac{\partial u}{\partial r} \right) + \frac{k_z}{\gamma_w} \left(\frac{\partial^2 u}{\partial z^2} \right) \quad (14a)$$

(2) when $(\sigma'_z, \varepsilon_z)$ is above the limit time line

$$-\frac{\kappa}{v(\sigma'_z - u)} \left(\frac{\partial \sigma'_z}{\partial t} - \frac{\partial u}{\partial t} \right) = \frac{k_r}{\gamma_w} \left(\frac{\partial^2 u}{\partial r^2} + \frac{1}{r} \frac{\partial u}{\partial r} \right) + \frac{k_z}{\gamma_w} \left(\frac{\partial^2 u}{\partial z^2} \right) + g(\sigma'_z, \varepsilon_z) \quad (14b)$$

where, σ'_z is the total vertical stress, $k'_r(r)$ and $k'_z(r)$ are the horizontal and vertical coefficients of permeability in the disturbed zone, respectively, and k_r and k_z are the horizontal and vertical coefficients of permeability in the intact zone, respectively. Referring to previous studies (e.g., Hansbo 1987, Bergado *et al.* 1991, Indraratna and Redana 1998a), horizontal and vertical permeability coefficients in the disturbed zone can be assumed equal (i.e., $k'_z(r) = k'_r(r)$).

Eqs. (13) and (14) are nonlinear partial differential equations simulating the consolidation process considering combined vertical and horizontal drainage conditions. The Crank-Nicholson finite difference scheme can be applied to solve these governing equations. Crank and Nicolson (1947) proposed a method that decreases the total volume of calculation, while the partial differential equation is being satisfied at the midpoint and is based on the trapezoidal rule in time. In this method, two steps are being used in partial differentials of pore water pressure over distance to stabilise the process more rapidly. Eqs. (15)-(22) are obtained after applying the Crank-Nicholson finite difference scheme to Eqs. (13) and (14).

For disturbed zone when $(\sigma'_z, \varepsilon_z)$ is below the limit time line

$$\begin{aligned} & \left(\frac{k'_{r,i,j,t}}{\gamma_w \Delta r^2} + \frac{k'_{z,i,j,t}}{\gamma_w \Delta z^2} + \frac{m_{v,i,j,t}}{\Delta t} \right) u_{i,j,t+1} + \frac{k'_{r,i,j,t}}{\gamma_w} \left(\frac{1}{4r\Delta r} - \frac{1}{2\Delta r^2} \right) u_{i-1,j,t+1} \\ & - \frac{k'_{r,i,j,t}}{\gamma_w} \left(\frac{1}{4r\Delta r} + \frac{1}{2\Delta r^2} \right) u_{i+1,j,t+1} - \frac{k'_{z,i,j,t}}{\gamma_w} \times \frac{1}{2\Delta z^2} u_{i,j-1,t+1} - \frac{k'_{z,i,j,t}}{\gamma_w} \times \frac{1}{2\Delta z^2} u_{i,j+1,t+1} \\ & = \frac{k'_{r,i,j,t}}{\gamma_w} \left[\frac{1}{2\Delta r^2} (u_{i-1,j,t} - 2u_{i,j,t} + u_{i+1,j,t}) + \frac{1}{4r\Delta r} (u_{i+1,j,t} - u_{i-1,j,t}) \right] \\ & + \frac{k'_{z,i,j,t}}{\gamma_w} \left[\frac{1}{2\Delta z^2} (u_{i,j-1,t} - 2u_{i,j,t} + u_{i,j+1,t}) \right] + \frac{m_{v,i,j,t}}{\Delta t} u_{i,j,t} + m_{v,i,j,t} \frac{\sigma_{z,i,j,t+1} - \sigma_{z,i,j,t}}{\Delta t} \end{aligned} \quad (15)$$

For disturbed zone when $(\sigma'_z, \varepsilon_z)$ is above the limit time line

$$\begin{aligned}
 & \left(\frac{k'_{r,j,t}}{\gamma_w \Delta r^2} + \frac{k'_{z,j,t}}{\gamma_w \Delta z^2} + \frac{m_{v,j,t}}{\Delta t} \right) u_{i,j,t+1} + \frac{k'_{r,j,t}}{\gamma_w} \left(\frac{1}{4r\Delta r} - \frac{1}{2\Delta r^2} \right) u_{i-1,j,t+1} \\
 & - \frac{k'_{r,j,t}}{\gamma_w} \left(\frac{1}{4r\Delta r} + \frac{1}{2\Delta r^2} \right) u_{i+1,j,t+1} - \frac{k'_{z,j,t}}{\gamma_w} \times \frac{1}{2\Delta z^2} u_{i,j-1,t+1} - \frac{k'_{z,j,t}}{\gamma_w} \times \frac{1}{2\Delta z^2} u_{i,j+1,t+1} \\
 & = \frac{k'_{r,j,t}}{\gamma_w} \left[\frac{1}{2\Delta r^2} (u_{i-1,j,t} - 2u_{i,j,t} + u_{i+1,j,t}) + \frac{1}{4r\Delta r} (u_{i+1,j,t} - u_{i-1,j,t}) \right] \\
 & + \frac{k'_{z,j,t}}{\gamma_w} \left[\frac{1}{2\Delta z^2} (u_{i,j-1,t} - 2u_{i,j,t} + u_{i,j+1,t}) \right] + \frac{m_{v,j,t}}{\Delta t} u_{i,j,t} + g_{i,j,t} + m_{v,j,t} \frac{\sigma_{z_{i,j,t+1}} - \sigma_{z_{i,j,t}}}{\Delta t}
 \end{aligned} \tag{16}$$

For intact zone when $(\sigma'_z, \varepsilon_z)$ is below the limit time line

$$\begin{aligned}
 & \left(\frac{k_{r,j,t}}{\gamma_w \Delta r^2} + \frac{k_{z,j,t}}{\gamma_w \Delta z^2} + \frac{m_{v,j,t}}{\Delta t} \right) u_{i,j,t+1} + \frac{k_{r,j,t}}{\gamma_w} \left(\frac{1}{4r\Delta r} - \frac{1}{2\Delta r^2} \right) u_{i-1,j,t+1} \\
 & - \frac{k_{r,j,t}}{\gamma_w} \left(\frac{1}{4r\Delta r} + \frac{1}{2\Delta r^2} \right) u_{i+1,j,t+1} - \frac{k_{z,j,t}}{\gamma_w} \times \frac{1}{2\Delta z^2} u_{i,j-1,t+1} - \frac{k_{z,j,t}}{\gamma_w} \times \frac{1}{2\Delta z^2} u_{i,j+1,t+1} \\
 & = \frac{k_{r,j,t}}{\gamma_w} \left[\frac{1}{2\Delta r^2} (u_{i-1,j,t} - 2u_{i,j,t} + u_{i+1,j,t}) + \frac{1}{4r\Delta r} (u_{i+1,j,t} - u_{i-1,j,t}) \right] \\
 & + \frac{k_{z,j,t}}{\gamma_w} \left[\frac{1}{2\Delta z^2} (u_{i,j-1,t} - 2u_{i,j,t} + u_{i,j+1,t}) \right] + \frac{m_{v,j,t}}{\Delta t} u_{i,j,t} + m_{v,j,t} \frac{\sigma_{z_{i,j,t+1}} - \sigma_{z_{i,j,t}}}{\Delta t}
 \end{aligned} \tag{17}$$

For intact zone when $(\sigma'_z, \varepsilon_z)$ is above the limit time line

$$\begin{aligned}
 & \left(\frac{k_{r,j,t}}{\gamma_w \Delta r^2} + \frac{k_{z,j,t}}{\gamma_w \Delta z^2} + \frac{m_{v,j,t}}{\Delta t} \right) u_{i,j,t+1} + \frac{k_{r,j,t}}{\gamma_w} \left(\frac{1}{4r\Delta r} - \frac{1}{2\Delta r^2} \right) u_{i-1,j,t+1} \\
 & - \frac{k_{r,j,t}}{\gamma_w} \left(\frac{1}{4r\Delta r} + \frac{1}{2\Delta r^2} \right) u_{i+1,j,t+1} - \frac{k_{z,j,t}}{\gamma_w} \times \frac{1}{2\Delta z^2} u_{i,j-1,t+1} - \frac{k_{z,j,t}}{\gamma_w} \times \frac{1}{2\Delta z^2} u_{i,j+1,t+1} \\
 & = \frac{k_{r,j,t}}{\gamma_w} \left[\frac{1}{2\Delta r^2} (u_{i-1,j,t} - 2u_{i,j,t} + u_{i+1,j,t}) + \frac{1}{4r\Delta r} (u_{i+1,j,t} - u_{i-1,j,t}) \right] \\
 & + \frac{k_{z,j,t}}{\gamma_w} \left[\frac{1}{2\Delta z^2} (u_{i,j-1,t} - 2u_{i,j,t} + u_{i,j+1,t}) \right] + \frac{m_{v,j,t}}{\Delta t} u_{i,j,t} + g_{i,j,t} + m_{v,j,t} \frac{\sigma_{z_{i,j,t+1}} - \sigma_{z_{i,j,t}}}{\Delta t}
 \end{aligned} \tag{18}$$

where

$$g_{i,j,t} = \frac{\psi_0}{vt_0} \left(\frac{\varepsilon_{z_0}^{ep} + \frac{\lambda}{v} \ln \left(\frac{\sigma_{i,j,t} - u_{i,j,t}}{\sigma'_{z_0}} \right) - \varepsilon_{i,j,t}}{\varepsilon_{cr_{i,j,t}}^{\text{limit}}} \right)^2 \exp \left(\frac{v}{\psi_0} \frac{\varepsilon_{z_0}^{ep} + \frac{\lambda}{v} \ln \left(\frac{\sigma_{i,j,t} - u_{i,j,t}}{\sigma'_{z_0}} \right) - \varepsilon_{i,j,t}}{1 + \frac{\varepsilon_{z_0}^{ep} + \frac{\lambda}{v} \ln \left(\frac{\sigma_{i,j,t} - u_{i,j,t}}{\sigma'_{z_0}} \right) - \varepsilon_{i,j,t}}{\varepsilon_{cr_{i,j,t}}^{\text{limit}}}} \right) \quad (19)$$

$$m_{v_{i,j,t}} = \frac{\kappa}{v(\sigma_{i,j,t} - u_{i,j,t})} \quad (20)$$

$$\varepsilon_{cr_{i,j,t}}^{\text{limit}} = \frac{e_{ref_{i,j,t}}}{1 + e_0} \quad (21)$$

$$e_{ref_{i,j,t}} = \left(\varepsilon_{z_{i,j,t}} - \frac{\lambda}{v} \ln \left(\frac{\sigma_{i,j,t} - u_{i,j,t}}{\sigma'_{z_0}} \right) \right) (1 + e_{0,i,j}) + e_{i,j,t} \quad (22)$$

where, the subscripts i and j represent the horizontal and vertical node coordinates as $i = 1, 2, 3, \dots, m$ and $j = 1, 2, 3, \dots, n$, respectively. Δz and Δr , are the mesh size in vertical and horizontal directions and Δt is the time step, as shown in Fig. 4.

As the numerical solutions for the partial differential equations are obtained using advanced matrix handling facilities in MATLAB software, the coordinates begin with 1 instead of 0 for the programming simplification. Permeability changes are taken into consideration as a function of void ratio changes. In other words, the slope of the straight line in $e - \log k$ space (permeability change index, c_k) is considered to calculate the permeability coefficient at each time step based on changes in the void ratio, as presented in Eq. (23).

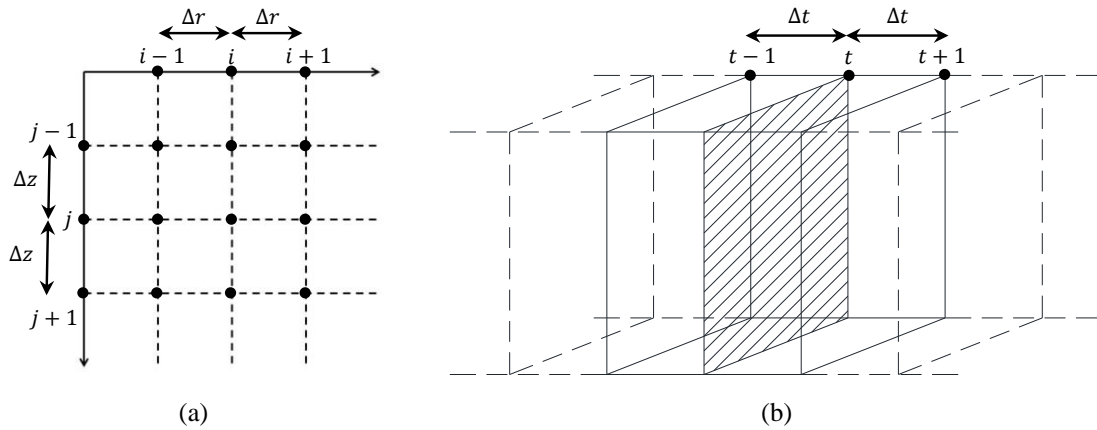


Fig. 4 (a) Location of finite difference nodes at any given time; (b) time steps

$$\Delta \log k_{i,j,t} = c_k \Delta e_{i,j,t} \quad (23)$$

To model the elastic visco-plastic behaviour of the soft soil, two different boundary conditions, which are the most frequent situations, are taken into consideration. Fig. 5(a) represents the situation when soft soil layer is sandwiched between two permeable layers at the top and bottom. Fig. 5(b) represents the situation when soft soil layer is surrounded by impervious layer at the bottom and highly permeable layer (drainage blanket) at the top.

The following boundary conditions (Eqs. (24) and (25)) can be applied for two-way drainage (Fig. 5(a)) and one-way drainage (Fig. 5(b)) conditions, respectively.

One-way drainage system

$$\begin{cases} u_{i,j,t} = \sigma_{z_{i,j,t+1}} + \sigma_{z_{i,j,t}} + u_{i,j,t-1} \\ u_{1,j,2:t} = u_{i,1,2:t} = u_{i,n,2:t} = 0 \end{cases} \quad (24)$$

Two-way drainage system

$$\begin{cases} u_{i,j,t} = \sigma_{z_{i,j,t+1}} - \sigma_{z_{i,j,t}} + u_{i,j,t-1} \\ u_{1,j,2:t} = u_{i,1,2:t} = 0 \\ u_{1,n,2:t} = u_{i,n-1,2:t} \end{cases} \quad (25)$$

Using the initial and boundary conditions and Eqs. (15)-(23), a system of equations involving tridiagonal square matrix is formed to obtain excess pore water pressures and strains. The average time dependant settlement in the influence area of a drain ($r = R$) at the top of the soil layer ($z = 0$) for a specific soil thickness ($z = H$) is given by

$$S_t = \int_{r=0}^{r=R} \int_{z=0}^{z=H} \frac{\varepsilon_z(r,z,t)}{R} dz dr \quad (26)$$

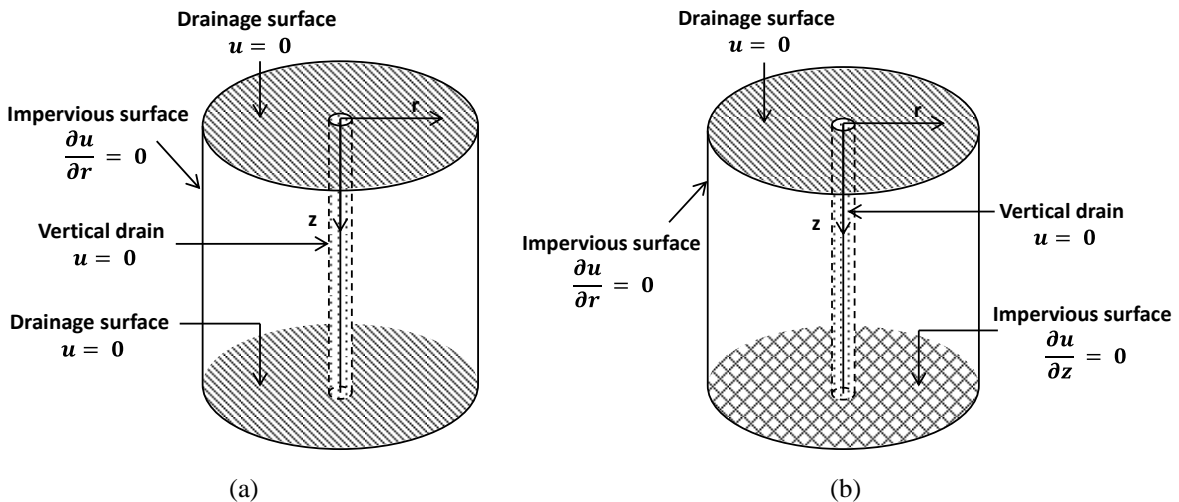


Fig. 5 Boundary conditions for (a) soil layer surrounded by two permeable layers (drains) at the top and bottom; (b) soil layer surrounded by impervious layer at the bottom and highly permeable layer (drainage blanket) at the top

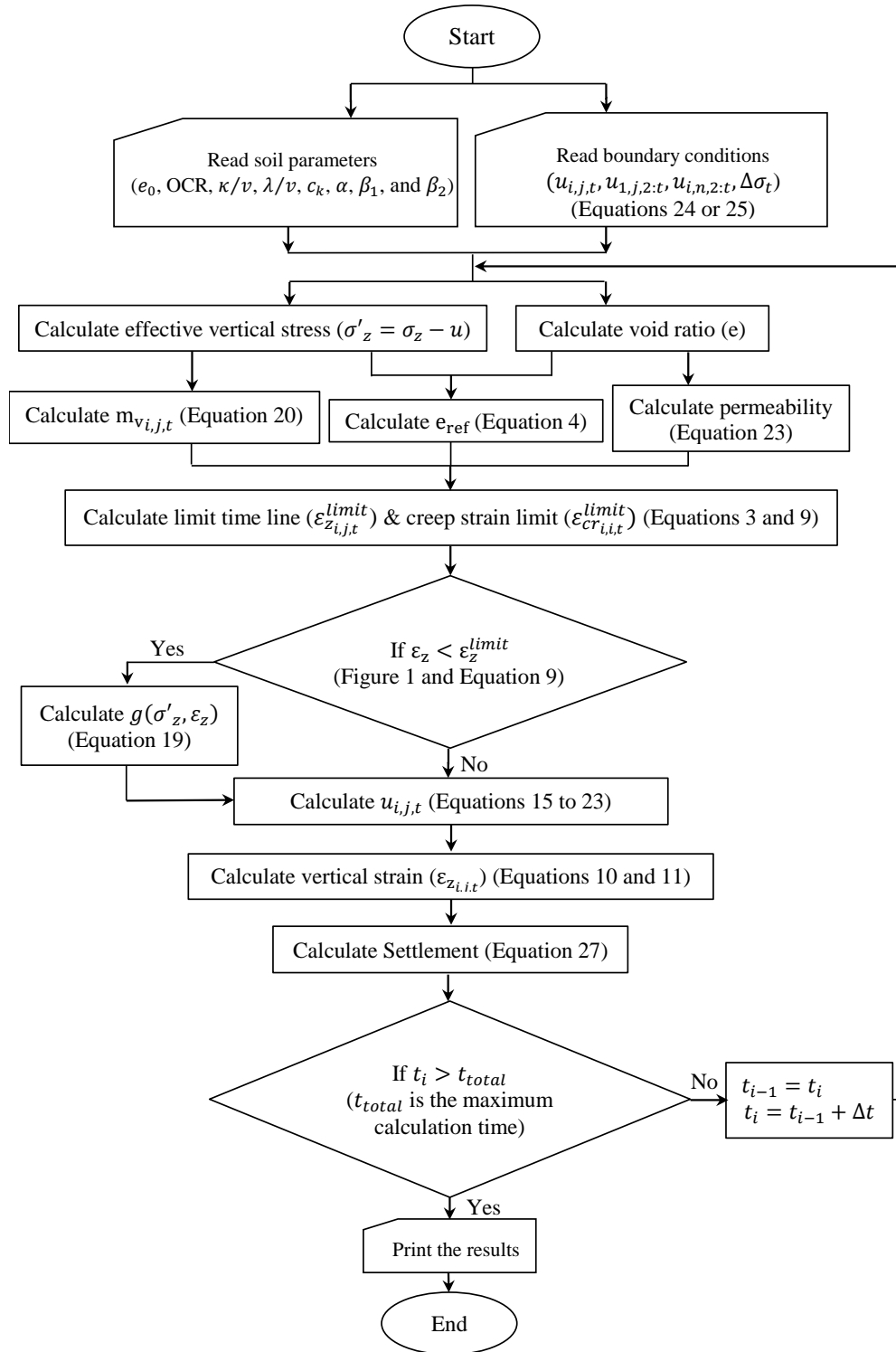


Fig. 6 Flowchart of the numerical analysis of vertical drains accelerated consolidation

Applying finite difference method to Eq. (26) provides the following equation to estimate settlement at time t .

$$S_t = \frac{H}{R} \sum_{i=1}^m \sum_{j=1}^n \varepsilon_{z_{i,j,t}} \tag{27}$$

where, the subscripts i and j represent the horizontal and vertical node coordinates.

Numerical solutions of Eqs. (15)-(23) are programmed in MATLAB for solution by a micro-computer. Fig. 6 depicts the flowchart of main steps in the numerical analysis.

5. Väsby test fill case study

The Swedish Geotechnical Institute (SGI) had designed and built Väsby test fill near Uplands Väsby village, 30 km north of Stockholm on the east coast of Sweden to study the long-term behaviour of Swedish clays and the suitability of the site for construction of an airport. Three test fills including one with vertical drains and two without vertical drains were built in Väsby area. The test fill with vertical drains has been selected to be discussed in this study.

As reported by Chang (1969, 1981), work on the test fill with vertical drains, which measured 30×30 m, was begun in 1945. The clay layer (Väsby post glacial clay) underlying this area was nearly 10 m thick. Prefabricated vertical drains installation depth and spacing were 5 m and 0.7 m, respectively. Settlement monitoring devices were established at the surface of the scraped ground and at the depths of 3.8 m and 5 m (see Fig. 7). Settlement markers consisted of a vertical steel rod, 19 mm in diameter, with a screw plate at its lower end. The gravel fill, with the unit weight of 17 kN/m³, was located to the height of 2.5 m on the top of the soft clay. A 0.8-m layer of gravel fill was removed half a year (i.e., 182 days) after completion of the surcharge placement.

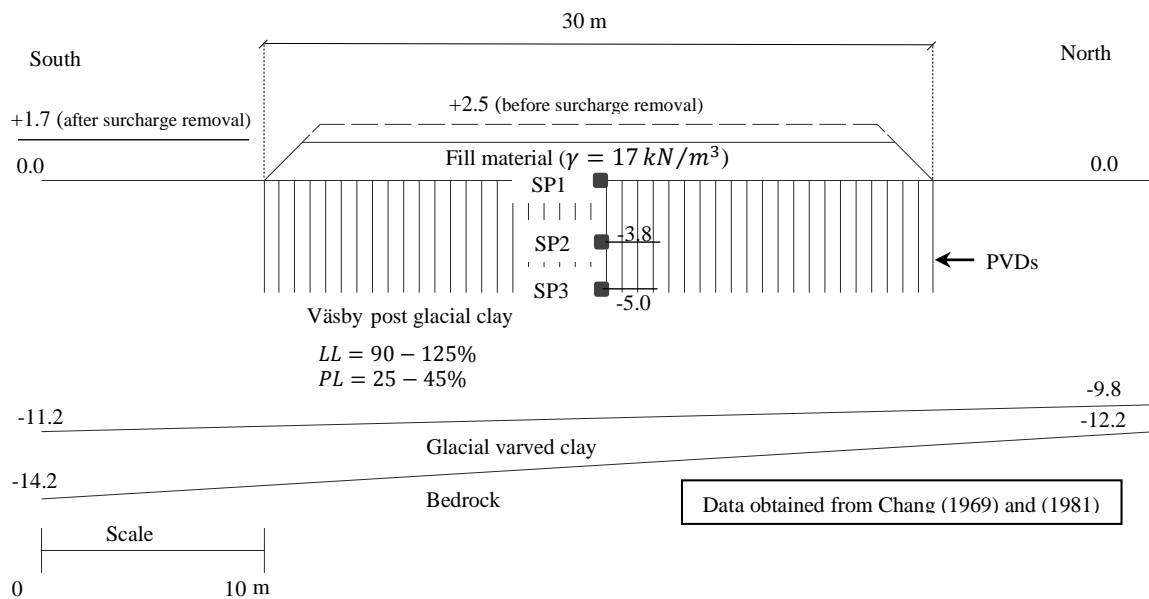
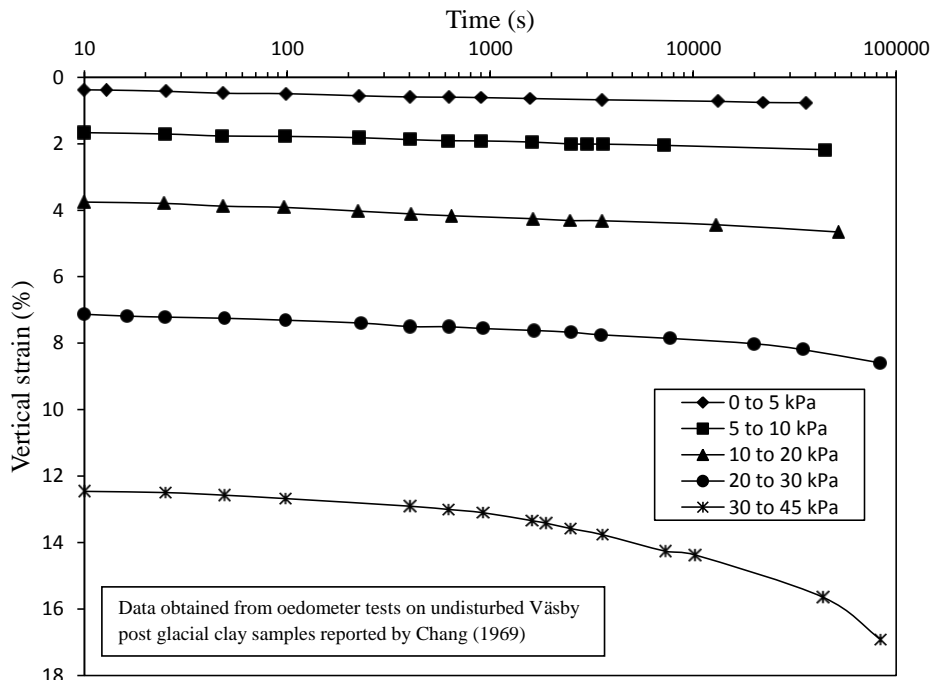
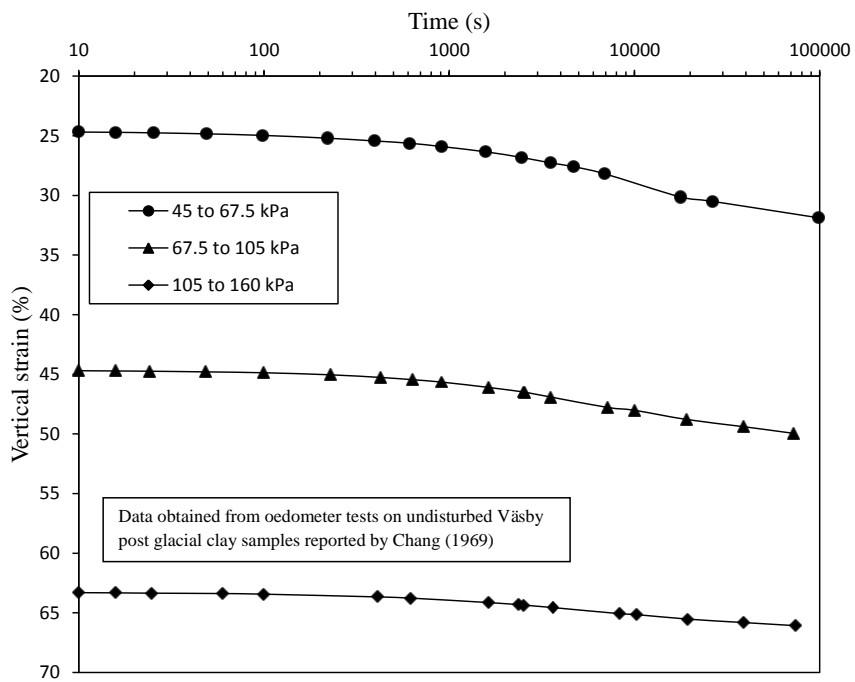


Fig. 7 Soil profile beneath the Väsby test fill



(a)



(b)

Fig. 8 (a) Consolidation tests results on Väsby post glacial clay samples for vertical stresses between 5 and 45 kPa; (b) Consolidation tests results on Väsby post glacial clay samples for vertical stresses between 45 and 160 kPa

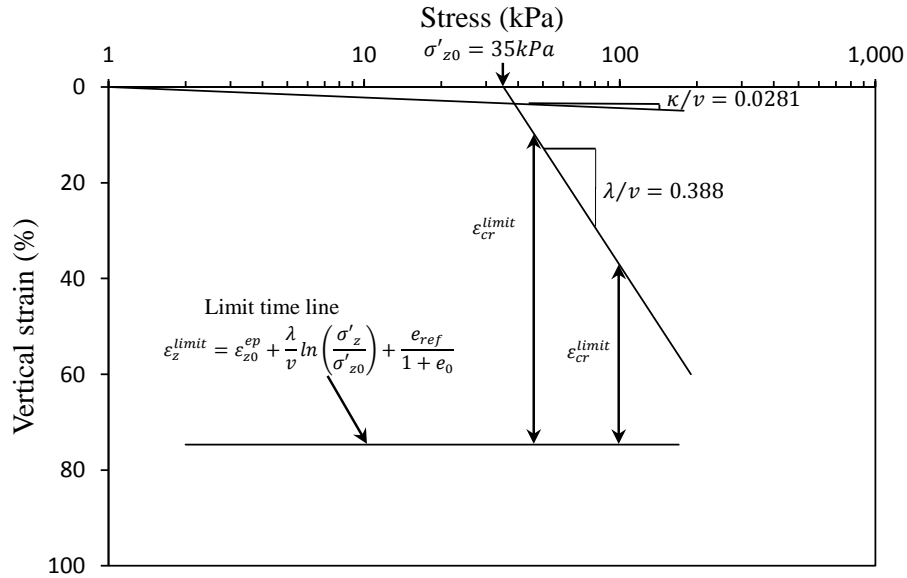


Fig. 9 Time dependant stress-vertical strain relationship for Väsby post glacial clay

Table 2 Adopted soil properties for Väsby post glacial clay

κ / v	λ / v	t_0 (s)	σ'_{z0} (kPa)	C_k	k_{r0} (m/s)	e_0	γ (kN/m ³)
0.0281	0.388	12000	35	0.785	7.2×10^{-10}	2.95	13.1–4.5

Table 3 Fitting parameters for disturbed zone permeability profile for Cases A-F

α	β_1	β_2	r_d (m)	r_s (m)	r_p (m)
0.25	0.6	0.75	0.15	0.05	0.1

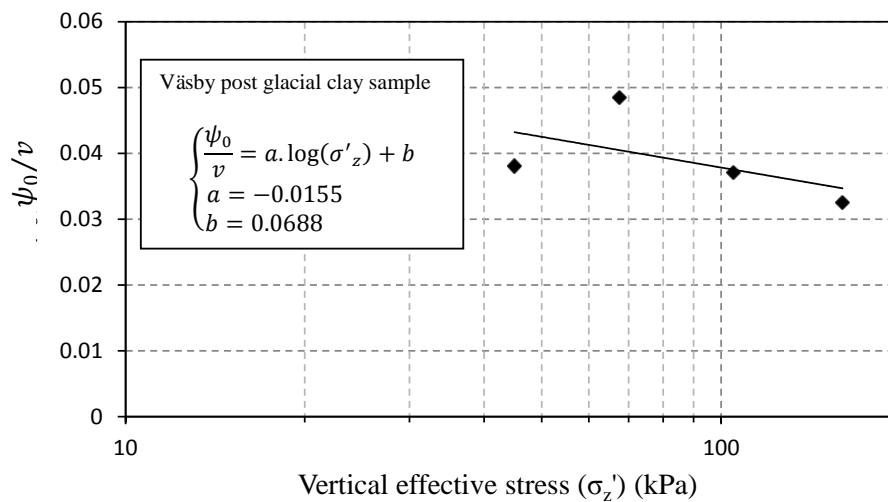


Fig. 10 Changes of ψ_0 / v versus vertical effective stress

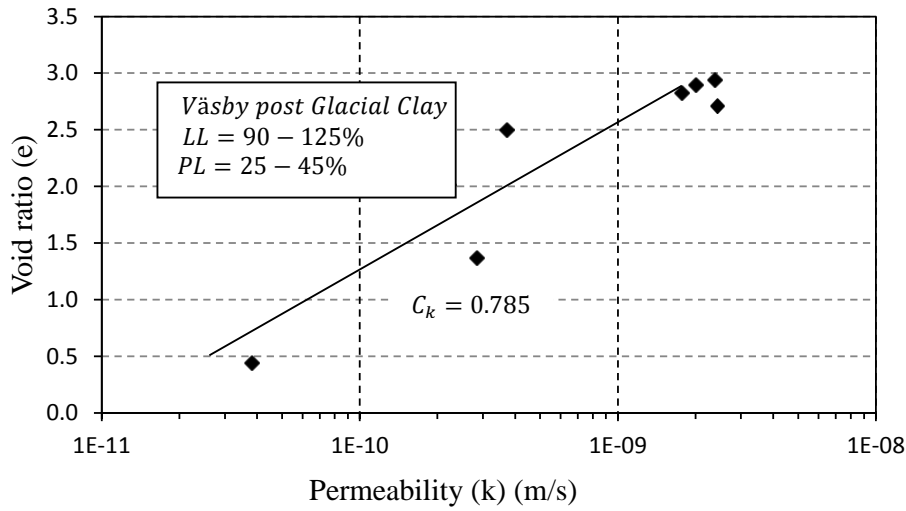


Fig. 11 Permeability changes versus void ratio

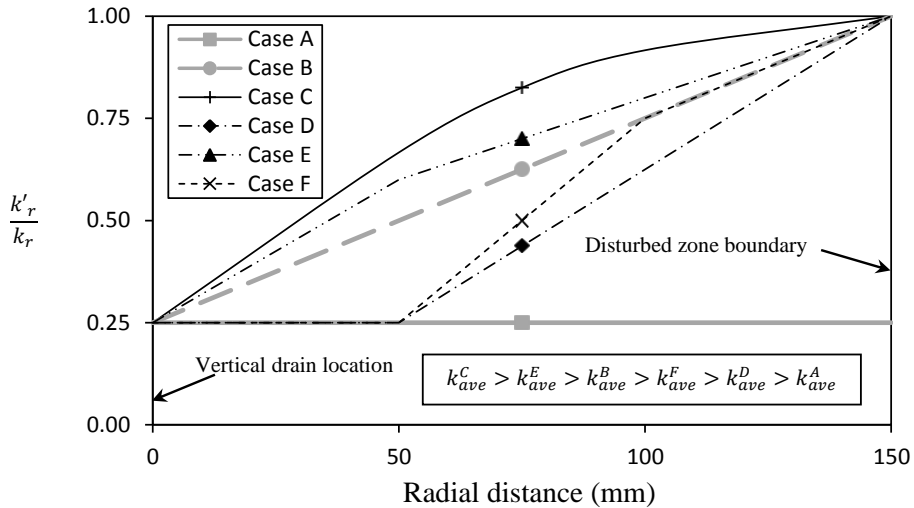


Fig. 12 Variations of initial permeability profile for Cases A to F

Referring to Fig. 10, in this case study, $\frac{\psi_0}{v}$ can be calculated as a function of the vertical effective stress for Väsby post glacial clay deposit $\left(\frac{\psi_0}{v} = -0.0155 \times \log(\sigma'_z) + 0.0688\right)$. Permeability of the soil at each loading stage in the oedometer test has been calculated using $k_r = C_v m_v \gamma_w$. For this purpose, Casagrande method (Casagrande and Fadum 1940) has been used to obtain the coefficient of the consolidation (C_v). Fig. 11 illustrates variation of the permeability coefficient with the void ratio for the undisturbed sample of Väsby Post glacial clay deposit adopted in this study. To investigate the influence of the permeability variation pattern in the

disturbed zone on the numerical predictions, all the permeability profiles as reported in Fig. 3 have been considered. Table 3 and Fig. 12 summarise the adopted parameters and pattern to simulate different permeability profiles in the disturbed zone.

Soil deformation during consolidation greatly depends on the initial state ($t = 0$) and boundary conditions. The thickness of the simulated soil deposit, which has overconsolidation ratio of 1.22 to 1.27, with both radial and vertical drainage systems is 5m with a drainage blanket on top (refer to Eq. (24) and Fig. 6). Time steps are assumed to be one tenth of a day with a total of 75000 steps, representing 20 years. Initial values of the excess pore water pressures (u_i), vertical effective stresses (σ'_{zi}), and vertical strains (ε_{zi}) are assumed to be 0, $(\gamma_{sat} - \gamma_w)z$, and 0, respectively.

6. Results and discussion

Fig. 13 shows the excess pore water pressure predictions at the depth of 2.6 m and in the middle of two vertical drains for different soil hydraulic conductivity profiles including Cases A to F. Comparing Figs. 12 and 13, it is evident that a lower average permeability in the disturbed zone results in a slower excess pore water pressure dissipation rate. For example, Cases A and C with lowest and highest average disturbed zone permeability ($k_{ave}^C > k_{ave}^E > k_{ave}^B > k_{ave}^F > k_{ave}^D > k_{ave}^A$), result in the highest and lowest remaining excess pore water pressures during the consolidation process, respectively. In addition, Cases D and F with comparable disturbed zone permeability values (see Fig. 12) demonstrate similar pattern of excess pore water pressure dissipation. As shown in Fig. 13, while the test embankment is being built, the excess pore water pressure keeps increasing and reaches its maximum value after 25 days, irrespective of the choice of the disturbed zone permeability profile. However, it can be observed that the maximum excess pore water pressure significantly depends on the choice of the permeability variation in the disturbed zone. As expected, the higher the average disturbed zone permeability is, the lower the maximum values of excess pore water pressure in the soil profile will be. For example, the maximum predicted excess pore water pressure values for Cases A to F, occurring at the end of fill placement period, are 36.5 kPa, 32.1 kPa, 27.9 kPa, 35.2 kPa, 30.7 kPa, and 34.9 kPa, respectively. In other words, Case A with constant initial disturbed zone permeability overestimates the maximum excess pore water pressure by 31% in comparison to Case C. In addition, as illustrated in Fig. 13, there is a rapid decrease in the excess pore water pressure induced by the partial removal of the fill material. This immediate reduction in the excess pore water pressure is approximately 13.5 kPa equal to the removal of 0.8 m of the gravel fill material with the unit weight of 17 kN/m³. Since the remaining excess pore water pressures in the soil deposit at the time of partial removal of the embankment are less than the removed fill material, negative excess pore water pressures are generated. Soon after completion of the unloading, the excess pore water pressures increase aiming to reach equilibrium followed by dissipation.

Fig. 14 shows the variations of excess pore water pressure with time for Case A. Obviously, excess pore water pressure is inversely related to radius. As explained earlier, during the construction of the embankment, excess pore water pressure increases and reaches its maximum value (i.e., 25 days) and then starts decreasing. Fig. 15 shows the comparison between excess pore water pressure values just before unloading for Cases A to F at the depth of 2.6 m. Obviously, excess pore water pressure is directly related to the distance from the vertical drain. In addition, the lower the average disturbed zone permeability is the higher the value of excess pore water pressure value in soil profile will be. For example, Case A with lower initial average permeability

shows 43% less excess pore water pressure in comparison to Case C, which has the highest initial average permeability.

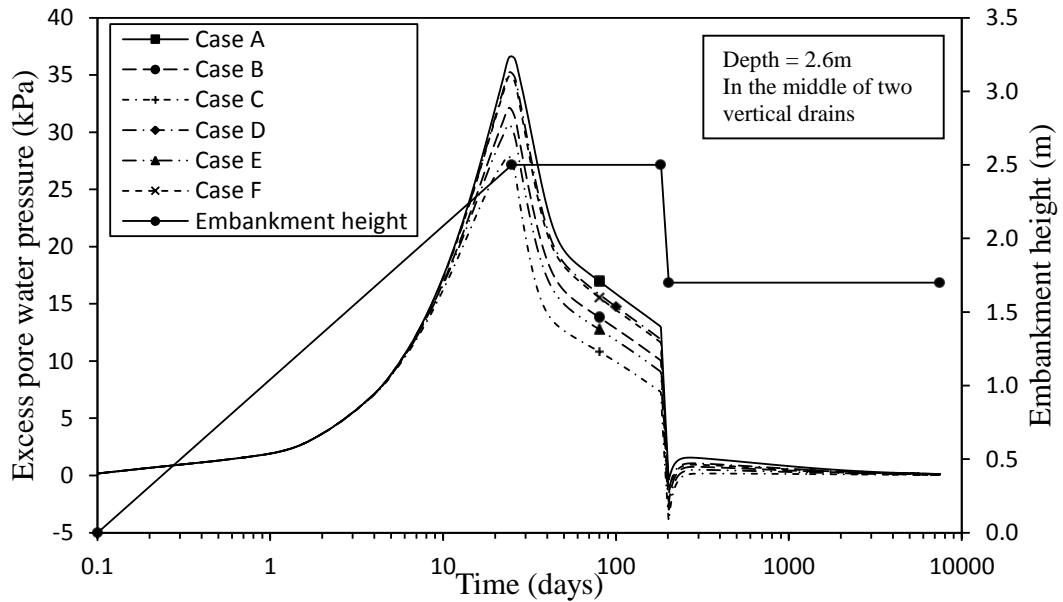


Fig. 13 Excess pore water pressure values predicted by developed code versus time for Cases A to F

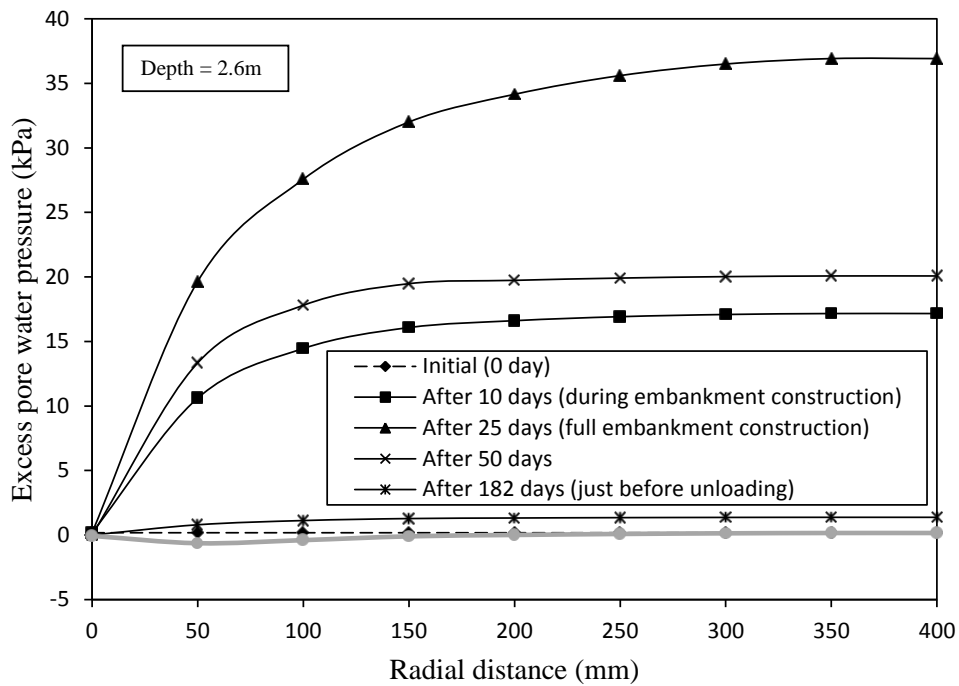


Fig. 14 Variations of excess pore water pressure with time for Case A

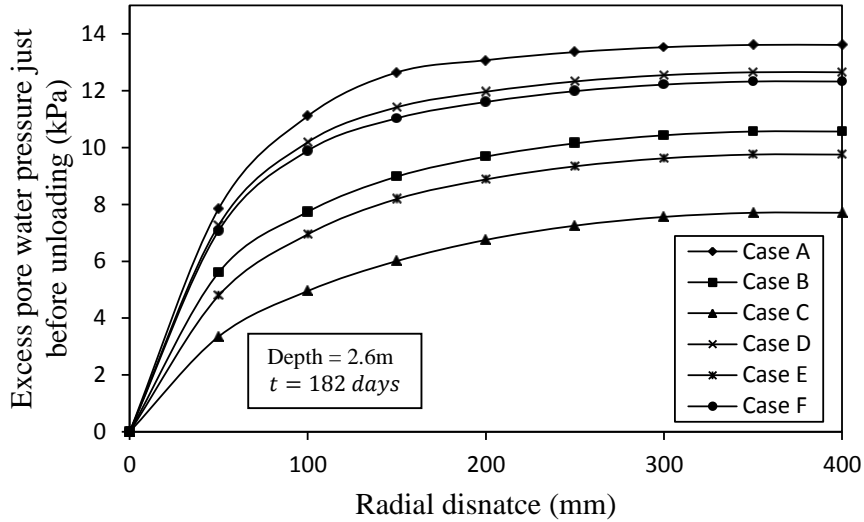


Fig. 15 Variations of the excess pore water pressure values just before unloading ($t = 182$ days) for Cases A to F

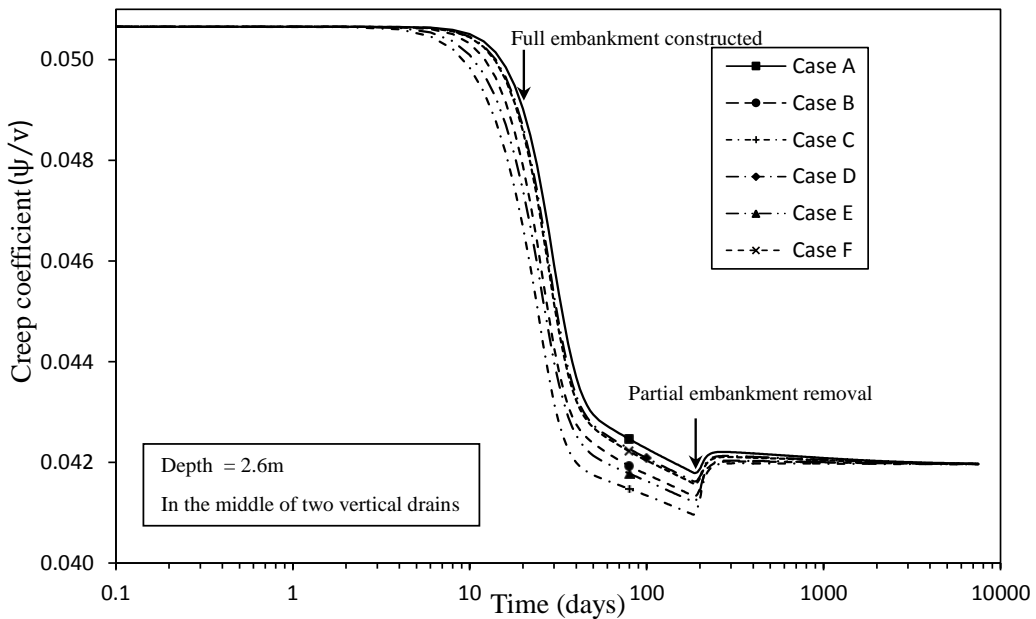


Fig. 16 Predicted creep coefficient (ψ/v) values versus time for Cases A to F

Fig. 16 depicts creep coefficient (ψ/v) variation with time at depth of 2.6 m in the middle of two vertical drains. Evidently, the creep coefficient changes with both time and choice of the disturbed zone permeability profile. For instant, the creep coefficient drops from 0.0505 to 0.0423 (16.2% reduction) between 10 days and 100 days, respectively (Case A). Since creep coefficient (ψ/v) is inversely related to the effective vertical stress (σ'_z) as shown in Fig. 10, lower effective

vertical stresses (or higher excess pore water pressures) cause higher creep coefficients. For example, as reported in Fig. 16, Case A (the lowest averaged permeability in the disturbed zone) and Case C (the highest average permeability in the disturbed zone) (Fig. 12), result in the highest and the lowest creep coefficients (ψ/v), respectively. As shown in Fig. 16, for the reported cases, influence of time on the creep coefficient is more pronounced than the effect of choice of disturbed zone permeability profile. Moreover, as observed in Fig. 16, there is a slight increase in the creep coefficient due to the partial removal of the fill material followed by a marginal increase with time, similar to the excess pore water pressure dissipation pattern reported in Fig. 13.

Fig. 17 shows variations of the predicted creep strain limit with time and choice of the disturbed zone permeability profile. Evidently, variations of the creep strain limit with time are more notable than with the permeability profile. For example, there is 67% reduction in the creep strain limit (from 2.33 to 0.77) from 10 days to 100 days (Case A), while this reduction is only up to 7.7% due to the choice of the permeability profile. Since, similar to the creep coefficient, the creep strain limit is also inversely related to the effective vertical stress (see Eqs. (3) and (4)), the lower equivalent permeability in the disturbed zone (resulting in a higher excess pore water pressures) leads to higher creep strain limit at any given time. In addition, unloading due to the partial removal of the embankment contributes to a slight increase in the creep strain limit followed by a gradual decrease similar to the creep coefficient variations.

Referring to Fig. 13, due to the simultaneous and professional increase in the total stresses and excess pore water pressures keep in the early stages of loading, the effective vertical stresses remain nearly unchanged. Thus, the creeps limit strain and the creep coefficient (Figs. 16 and 17), which are inversely proportional to the effective vertical stresses, remain unchanged in the early stages of loading.

Figs. 18 and 19 present the comparison between the predicted time dependent settlement and the field measurements for depths of 5 m and 3.8 m, respectively. To calculate the reported field

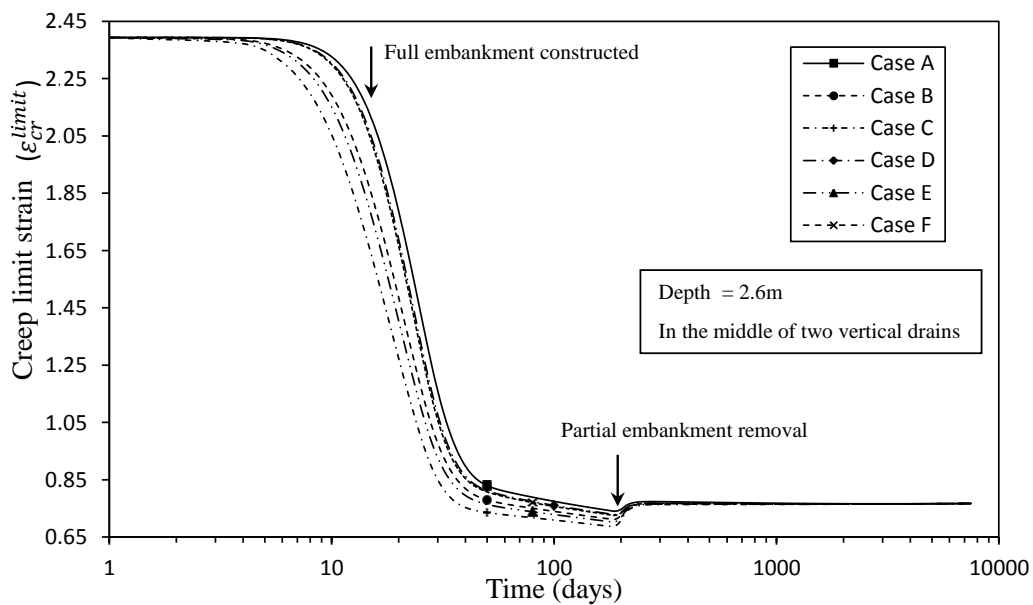


Fig. 17 Creep strain limit values predicted by the developed code versus time for Cases A to F

settlement values, the in situ settlement records at the settlement plate SP1 (located at the ground surface) and settlement plate SP2 (located at the depth of 5 m) were subtracted from the settlement records SP3 located 5 m deep (see Fig. 7). Numerical results show although settlement predictions converge after very long time (infinity), there are significant differences due to the choice of permeability variations in the disturbed zone. The predicted ground surface settlements just before the partial removal of the embankment for Cases A to F are 501 mm, 618 mm, 733 mm, 541 mm, 659 mm, and 552 mm, respectively, while, the in situ measurement is 545 mm. In other words, there is up to 46% difference in the predicted settlement after 182 days (just before unloading) due to the variation in the permeability profile in the disturbed zone. This difference for the settlement at depth 3.8 m (SP2-SP3) is 55%. Based on the settlement predictions and measurements reported in Figs. 18 and 19, although the settlement rate decreases significantly after unloading, settlement continues increasing due to visco-plastic deformation of the soil while insignificant excess pore water pressures are remaining. Comparing the measurements and predictions reported in Figs. 18 and 19 for this particular case study, numerical analysis predictions adopting Cases E and B with bilinear or linear variation profile of the initial permeability in the disturbed zone with radius, are in a reasonable agreement with the field measurements particularly after unloading.

Assuming the post construction settlement being the settlement occurring after the partial removal of the embankment, Fig. 20 shows the post construction settlement for 20 years. Evidently, the post construction settlement, which is mainly due to the viscous creep deformation, is influenced significantly by the permeability variations in the disturbed zone.

Fig. 21 shows the required time to achieve 500 mm of the ground surface settlement for all cases. Evidently, numerical results show that Case C with the highest average initial disturbed zone permeability needs 61% less time to achieve 500 mm settlement compared to Case A with the lowest average initial disturbed zone permeability. Consequently, selecting the permeability profile affects the decision of the proper time to remove the embankment considerably.

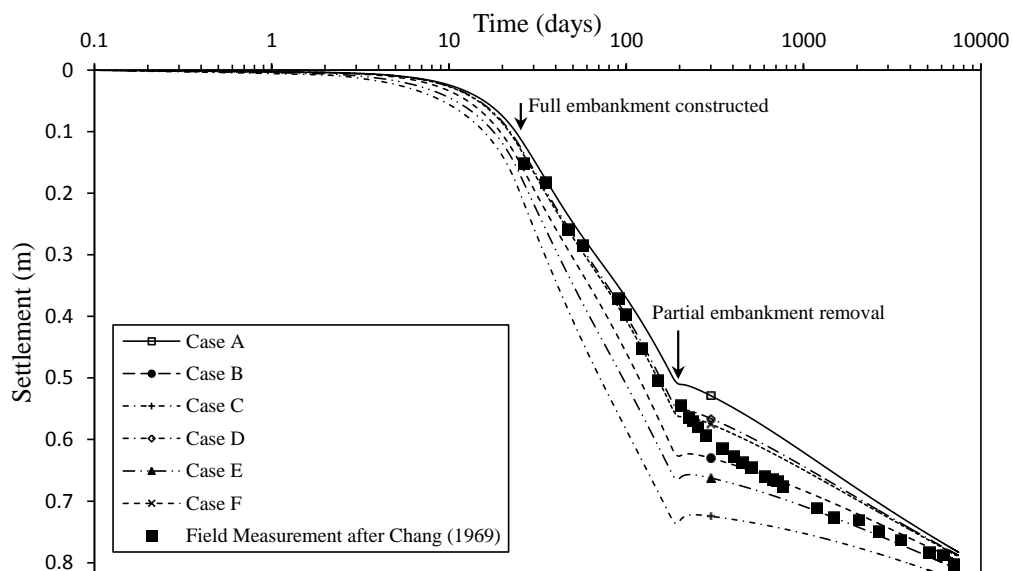


Fig. 18 Comparison of the settlement predictions for Cases A to F and the field measurements at the ground surface

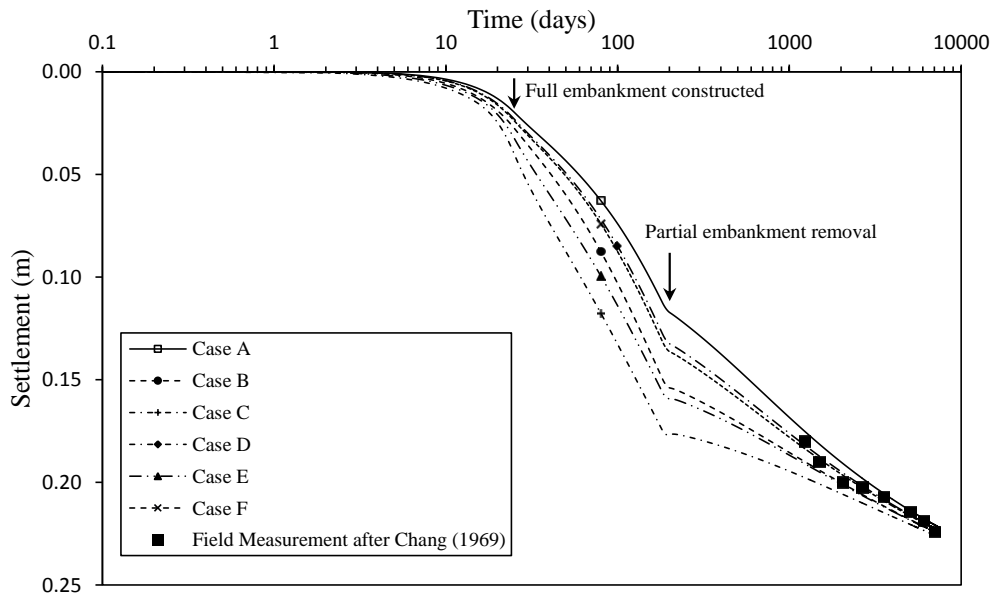


Fig. 19 Comparison between the settlement predictions for Cases A to F and the field measurements at 3.8 m depth

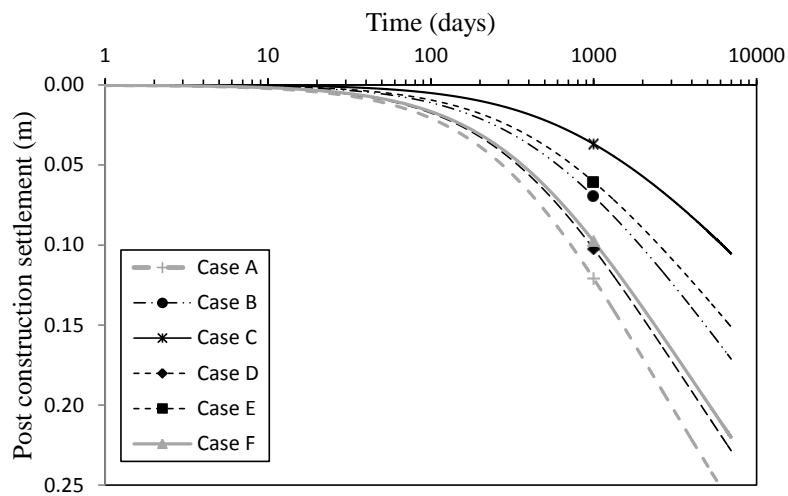


Fig. 20 Comparison between post construction settlement prediction for Cases A to F and the field measurement at the ground surface

Figs. 22 and 23 show the variations of permeability profile with time adopting Case A as the initial permeability profile. It can be concluded that the permeability coefficient, the permeability ratio $\left(\frac{k'_r}{k_r}\right)$ and the permeability variation pattern change with time. Obviously, the excess pore water pressure dissipation rate and consequently the void ratio reduction rate, while the excess pore water pressure in dissipating, decrease with the radius (distance from the vertical drain).

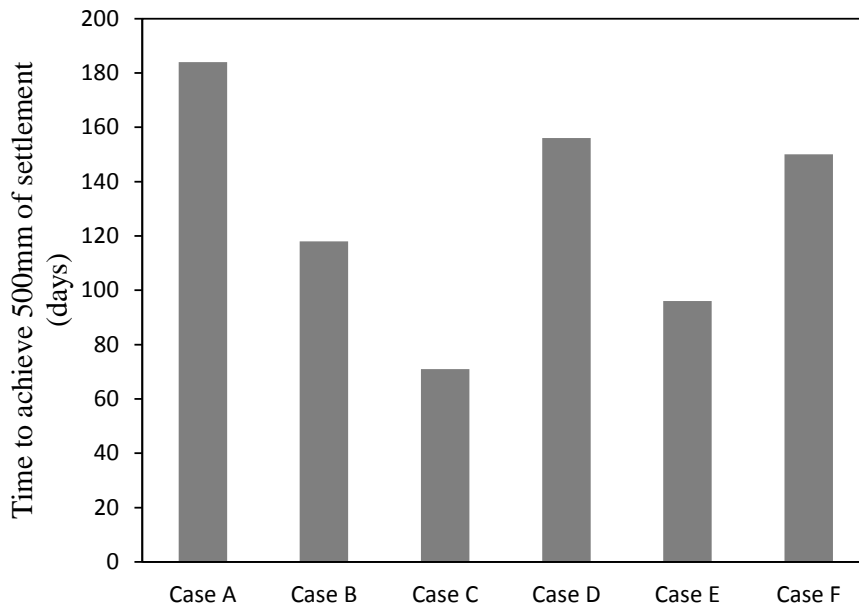


Fig. 21 The required time to achieve 500 mm of settlement for Cases A to F at the ground surface

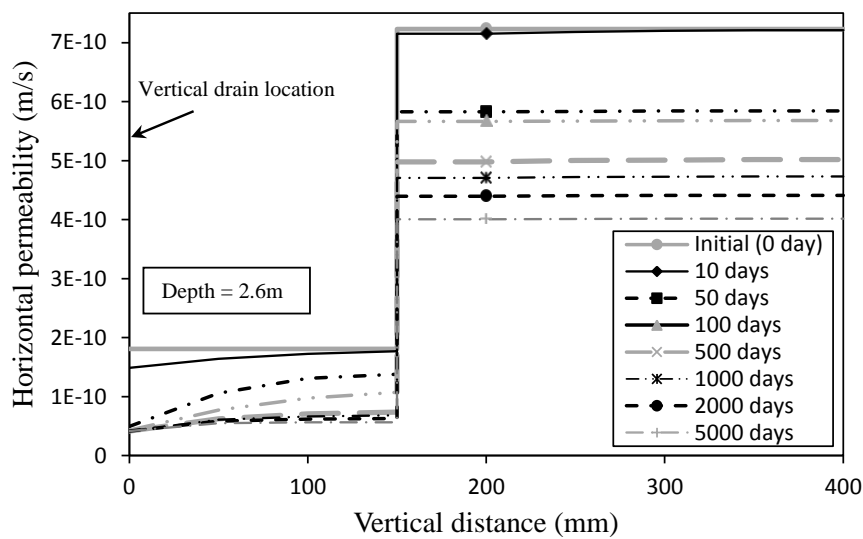


Fig. 22 Variations of permeability profile versus time for Case A

Therefore, the permeability decreases with time, while increases with radius. Thus, the pattern of the soil hydraulic conductivity variations does not keep similar to the initial pattern, in the process of consolidation and continuous ground settlement. For example, as Figs. 22 and 23 illustrate, although the uniform initial permeability coefficient and ratio were assumed for the disturbed zone, non-uniform/nonlinear variation exists during the consolidation process. According to Fig. 23 within the disturbed zone, while the excess pore water pressure is dissipating,

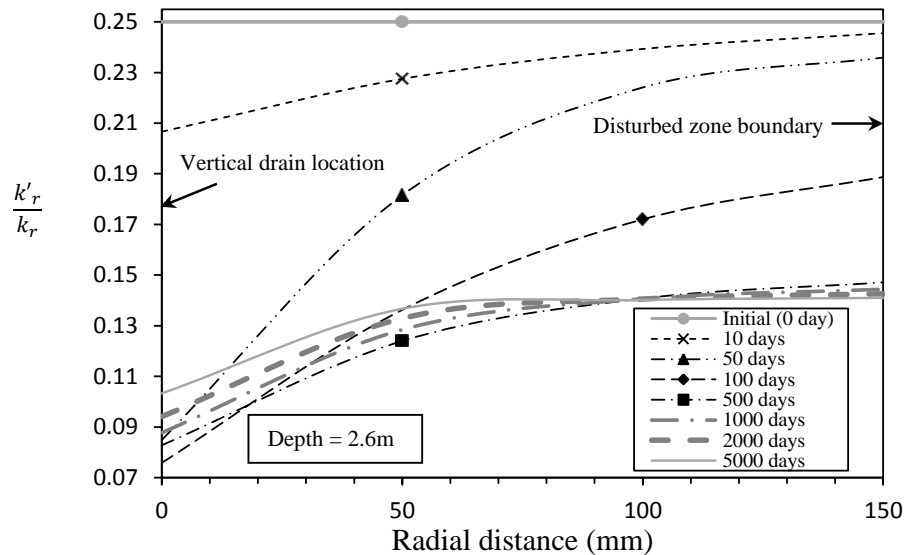


Fig. 23 Variations of permeability ratio with time in disturbed zone for Case A

the permeability ratio is decreasing following a direct relationship with radius. After excess pore water pressure dissipation, the void ratio reduction rate slows down (Fig. 16) and consequently, the permeability ratio starts increasing (Fig. 23).

7. Conclusions

Installation of vertical drains induces soil disturbance decreasing the in situ horizontal hydraulic conductivity in the vicinity of drains. The soil disturbance causes a slower rate of excess pore water pressure dissipation than what would be expected in the absence of the disturbance. Assessing the degree of change in the hydraulic conductivity in the disturbed zone to be used in the design procedure is a challenging task. According to available literature, six possible profiles of the initial hydraulic conductivity in the disturbed zone (Cases A, B, C, D, E, F) have been considered in this study. A numerical finite difference solution adopting an elastic visco-plastic model with nonlinear creep function incorporated in the consolidation equations has been developed to investigate the effects of soil disturbance on time dependant behaviour of soft soil deposits including vertical drains and preloading. The applied elastic visco-plastic model is based on the framework of modified Cam-Clay and nonlinear variations of the creep coefficient with the effective stress and time inclusion. In formulating the finite difference procedure, the Crank-Nicholson scheme has been used. In this method, two steps have been used in partial differentials of pore water pressure over distance to stabilise the process quicker. The developed numerical model considers the combined effects of soil creep, disturbed zone properties surrounding the vertical drains and nonlinear permeability variations during the consolidation process. Laboratory and field measurements from Väsby test fill including soft soil deposit improved with prefabricated vertical drains and preloading with staged loading and unloading process have been discussed and compared with the numerical predictions in this study.

Different initial hydraulic conductivity profiles in the disturbed zone result in various values of excess pore water pressure and effective vertical stresses at any given time in the soil profile. Consequently, the induced changes in the vertical effective stresses not only influence the consolidation process but also influence the creep coefficient and the creep strain limit resulting in different settlement rates at any given time. Therefore, selection of the initial hydraulic conductivity in the disturbed zone has a significant effect on choosing unloading time and thus on the post construction settlement. It is noted that since permeability is a function of void ratio, the assumed initial hydraulic conductivity profile does not stay the same during the consolidation process. In other words, permeability ratio and its variation pattern in the disturbed zone is significantly time dependant. It is worthy of note that, the creep coefficient and creep strain limit, regardless of initial hydraulic conductivity selection, change during loading and unloading and also while excess pore water pressure dissipation. Creep coefficient and creep strain limit are functions of the effective vertical stress and time. Consequently, during loading and unloading and while excess pore water pressure dissipation period, the effective vertical stress changes result in creep coefficient and creep strain limit variations.

The numerical results show that the proposed finite difference procedure incorporating elastic visco-plastic soil behaviour is appropriate for the consolidation analysis of preloading with vertical drains. The proposed solution can readily be used for layered soil deposits, time dependent loading and unloading, while considering combined effects of soil disturbance effects and visco-plastic behaviour.

References

- Azari, B., Fatahi, B. and Khabbaz, H. (2014), "Assessment of the elastic-viscoplastic behavior of soft soils improved with vertical drains capturing reduced shear strength of a disturbed zone", *Int. J. Geomech.* DOI: 10.1061/(ASCE)GM.1943-5622.0000448.
- Barden, L. (1965), "Consolidation of clay with non-linear viscosity", *Geotechnique*, **15**(4), 345-362.
- Barden, L. (1969), "Time-dependent deformation of normally consolidated clays and peats", *J. Soil Mech. Found. Div. ASCE*, **95**(1), 1-31.
- Barron, R.A. (1948), "Consolidation of fine-grained soils by drain wells", *T. Am. Soc. Civil Eng.*, **113**, 718-724.
- Basu, D. and Prezzi, M. (2007), "Effect of the smear and transition zones around prefabricated vertical drains installed in a triangular pattern on the rate of soil consolidation", *Int. J. Geomech. ASCE*, **7**(1), 34-43.
- Basu, D., Basu, P. and Prezzi, M. (2006), "Analytical solutions for consolidation aided by vertical drains", *Geomech. Geoeng.*, **1**(1), 63-71.
- Basu, D., Basu, P. and Prezzi, M. (2010), "Analysis of PVD-enhanced consolidation with soil disturbance", *Ground Improv.*, **163**(G4), 237-249.
- Bergado, D.T., Asakami, H., Alfaro, M.C. and Balasubramaniam, A.S. (1991), "Smear effects of vertical drains on soft Bangkok clay", *J. Geotech. Eng.*, **117**(10), 1509-1530.
- Bjerrum, L. (1967), "Engineering geology of norwegian normally consolidated marine clays as related to the settlement of buildings", *Geotechnique*, **17**(2), 83-118.
- Casagrande, A. and Fadum, R.E. (1940), *Notes on Soil Testing for Engineering Purposes*, Harvard Soil Mechanics, Volume 8, Cambridge, MA, USA.
- Chai, J. and Miura, N. (1999), "Investigation of factors affecting vertical drain behavior", *Journal of Geotech. Geoenviron. Eng.*, **125**(3), 216-226.
- Chai, J.C., Miura, N. and Sakajo, S. (1997), "A theoretical study on smear effect around vertical drain", *Proceedings of the 14th International Conference on Soil Mechanics and Foundation Engineering*,

- Hamburg, Germany, Volume 3, pp. 1581-1584.
- Chang, Y.C.E. (1969), "Long-term consolidation beneath the test fills at Vasby, Sweden", Ph.D. Thesis, University of Illinois, Champaign, IL, USA.
- Chang, Y.C.E. (1981), *Long-term Consolidation Beneath the Test Fills at Vasby, Sweden*, Swedish Geotechnical Institute, Linköping, Sweden.
- Crank, J. and Nicolson, P. (1947), "A practical method for numerical evaluation of solutions of partial differential equations of the heat-conduction type", *Mathematical Proceedings of the Cambridge Philosophical Society*, **43**(1), 50-67.
- Fatahi, B. and Tabatabaiefar, S. (2014), "Fully nonlinear versus equivalent linear computation method for seismic analysis of midrise buildings on soft soils", *Int. J. Geomech.*, **14**(4), 1-15.
- Fatahi, B., Fatahi, B., Le, T. and Khabbaz, H. (2013), "Small-strain properties of soft clay treated with fibre and cement", *Geosynth. Int.*, **20**(4), 286-300.
- Hansbo, S. (1981), "Consolidation of fine-grained soils by prefabricated drains", *Proceedings of the 10th International Conference on Soil Mechanics and Foundation Engineering*, Stockholm, Sweden, June, Balkema, Rotterdam, The Netherlands, pp. 677-682.
- Hansbo, S. (1987), "Design aspects of vertical drains and lime column installation", *Proceedings of the 9th Southeast Asian Geotechnical Conference*, Bangkok, Thailand, December, **2**(8), pp. 1-12.
- Hansbo, S. (1997), "Aspects of vertical drain design: Darcian or non-Darcian flow", *Geotechnique*, **47**(5), 983-992.
- Hawladar, B.C., Imai, G. and Muhunthan, B. (2002), "Numerical study of the factors affecting the consolidation of clay with vertical drains", *Geotext. Geomembr.*, **20**(4), 213-239.
- Hird, C.C. and Moseley, V.J. (2000), "Model study of seepage in smear zones around vertical drains in layered soil", *Geotechnique*, **50**(1), 89-97.
- Hird, C.C., Pyrah, I.C. and Russell, D. (1992), "Finite element modelling of vertical drains beneath embankment on soft ground", *Geotechnique*, **42**(3), 499-511.
- Ho, L.H., Fatahi, B. and Khabbaz, H. (2014), "Analytical solution for one-dimensional consolidation of unsaturated soils using eigenfunction expansion method", *Int. J. Numer. Anal. Method. Geomech.*, **38**(10), 1058-1077.
- Hokmabadi, A.S., Fatahi, B. and Samali, B. (2014a), "Assessment of soil-pile-structure interaction influencing seismic response of mid-rise buildings sitting on floating pile foundations", *Comput. Geotech.*, **55**(1), 172-186.
- Hokmabadi, A.S., Fatahi, B. and Samali, B. (2014b), "Seismic response of mid-rise buildings on shallow and end-bearing pile foundations in soft soil", *Soils Found.*, **54**(3), 345-363.
- Holtz, R.D. and Holm, B.G. (1973), "Excavation and sampling around some sand drains at Ska-Edeby, Sweden", *Proceedings of the 6th Scandinavian Geotechnical Meeting*, Trondheim, Norway, Norwegian Geotechnical Institute, pp. 79-85.
- Hong, H.P. and Shang, J.Q. (1998), "Probabilistic analysis of consolidation with prefabricated vertical drains for soil improvement", *Can. Geotech. J.*, **35**(4), 666-677.
- Indraratna, B. and Redana, I.W. (1998a), "Development of the smear zone around vertical band drains", *Proceedings of the ICE-Ground Improvement*, **2**(4), 165-178.
- Indraratna, B. and Redana, I.W. (1998b), "Laboratory determination of smear zone due to vertical drain installation", *Geotech. Geoenviron. Eng.*, **124**(2), 180-184.
- Indraratna, B., Rujikiatkamjorn, C. and Sathanathan, I. (2005), "Radial consolidation of clay using compressibility indices and varying horizontal permeability", *Can. Geotech. J.*, **42**(5), 1330-1341.
- Jamiolkowski, M., Lancellotta, R. and Wolski, W. (1983), "Precompression and speeding up consolidation", *Proceedings of the 8th European Conference on Soil Mechanics and Foundation Engineering*, Helsinki, Finland, Volume 2, pp. 1201-1226.
- Ladd, C.C. (1973), "Estimating settlements of structures supported on cohesive soils", Lecture Notes, Massachusetts Institute of Technology, Cambridge, MA, USA.
- Ladd, C.C., Foott, R., Ishihara, K., Schlosser, F. and Poulos, H.J. (1977), "Stress-deformation and strength characteristics", *Proceeding of 9th International Conference of Soil Mechanics, Foundation Engineering*,

- Tokyo, Japan, July, pp. 421-494.
- Le, T.M., Fatahi, B. and Khabbaz, H. (2012), "Viscous behaviour of soft clay and inducing factors", *Geotech. Geol. Eng.*, **30**(5), 1069-1083.
- Le, T.M., Fatahi, B. and Khabbaz, H. (2015), "Numerical optimisation to obtain elastic viscoplastic model parameters for soft clay", *Int. J. Plasticity*, **65**, 1-21.
- Lo, D.O.K. and Mesri, G. (1994), *Settlement of Test Fills for Chek Lap Kok Airport*, In: Vertical and Horizontal Deformations of Foundations and Embankments, (Edited by A.T. Yeung and G. Fealio), American Society of Civil Engineers: New York, NY, USA, pp. 1082-1099.
- Madhav, M.R., Park, Y.M. and Miura, N. (1993), "Modelling and study of smear zones around band shaped drains", *Soils Found.*, **33**(4), 135-147.
- Mesri, G. (1986), "Postconstruction settlement of an expressway built on peat by precompression", *Can. Geotech. J.*, **22**(3), 308-312.
- Mesri, G. (2001), "Primary compression and secondary compression: Soil behavior and soft ground construction", *Geotechnical Specification*, **119**, 122-166.
- Mesri, G. and Feng, T.W. (1991), "Surcharging to reduce secondary settlements", *Proceedings of the International Conference on Geotechnical Engineering for Coastal Development – Theory of Practice*, Yokohama, Japan, September, pp. 359-364.
- Mesri, G. and Rokhsar, A. (1994), "Theory of consolidation for clays", *J. Geotech. Eng. Div., ASCE*, **100**, 889-904.
- Mesri, G., Rokhsar, A. and Bohor, B.F. (1975), "Composition and compressibility of typical samples of Mexico City clay", *Geotechnique*, **25**(3), 527-554.
- Mesri, G., Shahien, M. and Feng, T.W. (1995), "Compressibility parameters during primary consolidation", *Proceedings of the International Symposium on Compression and Consolidation of Clayey Soils*, Hiroshima, Japan, May, Volume 2, pp. 1021-1037.
- Mitchell, J.K. (1956), "The fabric of natural clays and its relation to engineering properties", *Proceedings of the 35th Annual Meeting of the Highway Research Board*, Washington, D.C., USA, January, Volume 35, pp. 693-713.
- Nash, D.F.T. and Ryde, S.J. (2001), "Modelling consolidation accelerated by vertical drains in soils subject to creep", *Geotechnique*, **51**(3), 257-273.
- Nguyen, L.D., Fatahi, B. and Khabbaz, H. (2014), "A constitutive model for cemented clays capturing cementation degradation", *Int. J. Plasticity*, **56**, 1-18.
- Onoue, A., Ting, N.H., Germaine, J.T. and Whitman, R.V. (1991), "Permeability of disturbed zone around vertical drains", *Proceedings of the Geotechnical Engineering Congress*, Boulder, CO, USA, June, pp. 879-890.
- Qin, A., Sun, D.A. and Zhang, J. (2014), "Semi-analytical solution to one-dimensional consolidation for viscoelastic unsaturated soils", *Comput. Geotech.*, **62**, 110-117.
- Parsa-Pajouh, A., Fatahi, B., Vincent, P. and Khabbaz, H. (2014), "Analyzing consolidation data to predict smear zone characteristics induced by vertical drain installation for soft soil improvement", *Geomech. Eng., Int. J.*, **7**(1), 105-131.
- Rendulic, L. (1935), *Der hydrodynamische Spannungsausgleich in zentral entwässerten Tonzylindern*, *Wasserwirtsch-Wassertechnik*, Volume 2, 250-253 & 269-273.
- Rendulic, L. (1936), *Porenziffer und Porenwasserdruck in Tonen*, Springer, pp. 559-564.
- Rujikiatkamjorn, C. and Indraratna, B. (2009), "Design procedure for vertical drains considering a linear variation of lateral permeability within the smear zone", *Can. Geotech. J.*, **46**(3), 270-280.
- Sharma, J.S. and Xiao, D. (2000), "Characterization of a smear zone around vertical drains by large-scale laboratory tests", *Can. Geotech. J.*, **37**(6), 1265-1271.
- Shen, W.Q., Shao, J.F., Kondo, D. and Gatmiri, B. (2012), "A micro-macro model for clayey rocks with a plastic compressible porous matrix", *Int. J. Plasticity*, **36**, 64-85.
- Suklje, L. (1957), "The analysis of the consolidation process by the isotache method", *Proceeding of 4th International Conference of Soil Mechanics and Foundation Engineering*, London, UK, August, Volume 1, pp. 200-206.

- Tabatabaiefar, S. and Fatahi, B. (2014), "Idealisation of soil-structure system to determine inelastic seismic response of mid-rise building frames", *Soil Dyn. Earthq. Eng.*, **66**(1), 339-351.
- Tabatabaiefar, S., Fatahi, B. and Samali, B. (2013b), "Seismic behavior of building frames considering dynamic soil-structure interaction", *Int. J. Geomech.*, **13**(4), 409-420.
- Tabatabaiefar, S., Fatahi, B. and Samali, B. (2013a), "Lateral seismic response of building frames considering dynamic soil-structure interaction effects", *Struct. Eng. Mech., Int. J.*, **45**(3), 311-321.
- Terzaghi, K. (1925), *Erdbaumechanik auf bodenphysikalischer Grundlage*, Deuticke: Vienna.
- Terzaghi, K. (1941), *Undisturbed Clay Samples and Undisturbed Clays*, Harvard University, Cambridge, MA, USA.
- Walker, R. and Indraratna, B. (2006), "Vertical drain consolidation with parabolic distribution of permeability in smear zone", *J. Geotech. Geoenviron. Eng.*, **132**(7), 937-941.
- Xie, K., Li, C., Liu, X. and Wang, Y. (2012), "Analysis of one-dimensional consolidation of soft soils with non-Darcian flow caused by non-Newtonian liquid", *J. Rock Mech. Geotech. Eng.*, **4**(3), 250-257.
- Yin, J.H. (1990), "Constitutive modelling of time-dependent stress-strain behaviour of soils", Ph.D. Thesis, University of Manitoba, Winnipeg, Manitoba, Canada.
- Yin, J.H. (1999), "Non-linear creep of soils in Oedometer tests", *Geotechnique*, **49**(5), 669-707.
- Yin, J.H. and Graham, J. (1989), "Viscous-elastic-plastic modelling of one dimensional time-dependent behaviour of clays", *Can. Geotech. J.*, **26**(2), 199-209.
- Yin, J.H. and Graham, J. (1994), "Equivalent times and one-dimensional elastic viscoplastic modelling of time-dependent stress-strain behaviour of clays", *Can. Geotech. J.*, **31**(1), 42-52.
- Yin, J.H., Zhu, G. and Graham, J. (2002), "A new elastic viscoplastic model for time-dependant behaviour of normally and overconsolidated clays: Theory and verification", *Can. Geotech. J.*, **39**(1), 157-173.
- Zhu, G. and Yin, J.H. (2000), "Finite element consolidation analysis of soils with vertical drain", *Int. J. Numer. Anal. Method. Geomech.*, **24**(4), 337-366.

Nomenclature

C_c	conventional compression index
C_r	conventional recompression index (unloading and reloading data)
c_k	permeability change index
c_v	coefficient of consolidation
e_0	initial void ratio
e_{ref}	void ratio at effective stress equal to σ'_z on reference time line
e_z	void ratio for a particular applied effective stress σ'_z
e_{EOP}	void ratio when the excess pore water pressure has fully dissipated
i	horizontal node coordinator
j	vertical node coordinator
k_0	initial permeability
k_{ave}^A	average disturbed zone permeability for Case A
k_{ave}^B	average disturbed zone permeability for Case B
k_{ave}^C	average disturbed zone permeability for Case C
k_{ave}^D	average disturbed zone permeability for Case D
k_{ave}^E	average disturbed zone permeability for Case E
k_{ave}^F	average disturbed zone permeability for Case F
$k'_r(r)$	coefficients of permeability for horizontal direction for disturbed zone
$k'_z(r)$	coefficients of permeability for vertical direction for disturbed zone
k_r	coefficients of permeability for horizontal direction for intact zone
k_z	coefficients of permeability for vertical direction for intact zone
H	layer depth
r	radial coordinate
r_d	disturbed zone radius
r_p	partial disturbed zone radius
r_s	smear zone radius
R	disturbed zone radius
S_t	average total settlement
t	time
t_0	curve-fitting parameter related to the choice of reference time line

t_e	equivalent time
t_{total}	maximum calculation time
u	excess pore water pressure
v	specific volume ($1 + e$)
z	vertical coordinate
α	permeability ratio parameter
β_1	permeability ratio parameter
β_2	permeability ratio parameter
γ_{sat}	saturated unit weight of soil
γ_w	unit weight of water
Δr	radial distance increment
Δt	time step
Δz	vertical distance increment
ε_z	soil vertical strain
ε_z^e	vertical strain at stress level σ'_z
ε_{z0}^e	vertical strain at $\sigma'_z = \sigma'_u$
ε_z^{ep}	reference time line strain
ε_{z0}^{ep}	vertical strain at $\sigma'_z = \sigma'_{z0}$
ε_{cr}^{limit}	creep strain limit
ε_z^{limit}	strain limit
ε_z^{vp}	creep compression strain
$\frac{k}{v}$	material parameter describing the elastic stiffness of the soil
$\frac{\lambda}{v}$	material property describing the elastic-plastic stiffness of the soil
σ'_u	unit stress
σ'_{z0}	material property
$\frac{\psi_0}{v}$	initial creep coefficient